Central Iowa Expo Pavement Project: Phase IV Performance Assessment Experimental Test Plan

Final Report
May 2023

IOWA STATE UNIVERSITY
Institute for Transportation

Sponsored by
Iowa Highway Research Board
(IHRB Project TR-817)
Iowa Department of Transportation
(InTrans Project 22-830)

About the Institute for Transportation

The mission of the Institute for Transportation (InTrans) at Iowa State University is to save lives and improve economic vitality through discovery, research innovation, outreach, and the implementation of bold ideas.

Iowa State University Nondiscrimination Statement

Iowa State University does not discriminate on the basis of race, color, age, ethnicity, religion, national origin, pregnancy, sexual orientation, gender identity, genetic information, sex, marital status, disability, or status as a US veteran. Inquiries regarding nondiscrimination policies may be directed to the Office of Equal Opportunity, 3410 Beardshear Hall, 515 Morrill Road, Ames, Iowa 50011, telephone: 515-294-7612, hotline: 515-294-1222, email: eooffice@iastate.edu.

Disclaimer Notice

The contents of this report reflect the views of the authors, who are responsible for the facts and the accuracy of the information presented herein. The opinions, findings and conclusions expressed in this publication are those of the authors and not necessarily those of the sponsors.

The sponsors assume no liability for the contents or use of the information contained in this document. This report does not constitute a standard, specification, or regulation.

The sponsors do not endorse products or manufacturers. Trademarks or manufacturers' names appear in this report only because they are considered essential to the objective of the document.

Iowa DOT Statements

Federal and state laws prohibit employment and/or public accommodation discrimination on the basis of age, color, creed, disability, gender identity, national origin, pregnancy, race, religion, sex, sexual orientation or veteran's status. If you believe you have been discriminated against, please contact the Iowa Civil Rights Commission at 800-457-4416 or the Iowa Department of Transportation affirmative action officer. If you need accommodations because of a disability to access the Iowa Department of Transportation's services, contact the agency's affirmative action officer at 800-262-0003.

The preparation of this report was financed in part through funds provided by the Iowa Department of Transportation through its "Second Revised Agreement for the Management of Research Conducted by Iowa State University for the Iowa Department of Transportation" and its amendments.

The opinions, findings, and conclusions expressed in this publication are those of the authors and not necessarily those of the Iowa Department of Transportation.

Front Cover Image Credits

White, D. J., P. Vennapusa, and T. Cackler. 2019. *In Situ Modulus Measurement Using Automated Plate Load Testing for Statewide Mechanistic-Empirical Design Calibration*. Report No. ST-003. Iowa Department of Transportation, Ames, IA.

CENTRAL IOWA EXPO PAVEMENT PROJECT: PHASE IV PERFORMANCE ASSESSMENT EXPERIMENTAL TEST PLAN

Final Report
May 2023

Principal Investigator
Jeramy C. Ashlock, Ph.D., Associate Professor
Institute for Transportation, Iowa State University

Research Team Members
David J. White, Ph.D., P.E., President and CEO
Pavana Vennapusa, Ph.D., P.E., Engineering Services Manager
John Puls, P.E., Business Unit Leader
Ingios Geotechnics, Inc.

Authors
Jeramy Ashlock, David White, Pavana Vennapusa, John Puls

Sponsored by
Iowa Highway Research Board and
Iowa Department of Transportation
(IHRB Project TR-817)

Preparation of this report was financed in part
through funds provided by the Iowa Department of Transportation
through its Research Management Agreement with the
Institute for Transportation
(InTrans Project 22-830)

A report from
Institute for Transportation
Iowa State University
2711 South Loop Drive, Suite 4700
Ames, IA 50010-8664
Phone: 515-294-8103 / Fax: 515-294-0467
https://intrans.iastate.edu

Technical Report Documentation Page

1. Report No.	2. Government Accession No.	3. Recipient's Catalog No.	
IHRB Project TR-817			
4. Title and Subtitle Central Iowa Expo Pavement Project: Phase IV Performance Assessment Experimental Test Plan		**5. Report Date** May 2023 **6. Performing Organization Code**	
7. Author(s) Jeramy Ashlock (orcid.org/0000-0003-0677-9900), David White (orcid.org/0000-0003-0802-1167), Pavana Vennapusa (orcid.org/0000-0001-9529-394X), John Puls (orcid.org/0000-0001-5435-4021)		**8. Performing Organization Report No.** InTrans Project 22-830	
9. Performing Organization Name and Address Institute for Transportation Iowa State University 2711 South Loop Drive, Suite 4700 Ames, IA 50010-8664		**10. Work Unit No. (TRAIS)** **11. Contract or Grant No.**	
12. Sponsoring Organization Name and Address Iowa Highway Research Board Iowa Department of Transportation 800 Lincoln Way Ames, IA 50010		**13. Type of Report and Period Covered** Final Report **14. Sponsoring Agency Code** IHRB Project TR-817	
15. Supplementary Notes Visit https://intrans.iastate.edu for color pdfs of this and other research reports.			

16. Abstract

Approximately 4.8 miles of roadways at the Central Iowa Expo facility in Boone, Iowa, were reconstructed in 2012 as part of Iowa Highway Research Board (IHRB) project TR-671. The project included three phases encompassing construction and field testing to assess the performance of several pavement foundation technologies. The Iowa Department of Transportation (DOT) has approved a Phase IV project to assess the long-term performance of the pavements evaluated in Phases I through III.

This report provides recommendations for two experimental test plan alternatives for Phase IV, one outlining a minimum recommended scope and another outlining a comprehensive scope to more precisely quantify differences among test sections. The overall goal of the testing program is direct measurement of not only the in situ mechanistic input parameters necessary for AASHTOWare Pavement ME Design but also the impacts of seasonal variations in the measurement values.

The report includes a statistical analysis of the data from Phases I through III and, based on this analysis, recommendations regarding the specific sections to test as well as the number and type of tests to perform. The methods proposed for Phase IV field testing include automated plate load testing, core hole permeability testing, and dynamic cone penetrometer testing. The report also summarizes engineering measurement values to be obtained for each test. Tests will be conducted in fall 2023, spring 2024, fall 2024, and spring 2025.

17. Key Words	18. Distribution Statement		
in situ testing—low volume roads—performance assessment—plate load testing—soil stabilization	No restrictions.		
19. Security Classification (of this report)	**20. Security Classification (of this page)**	**21. No. of Pages**	**22. Price**
Unclassified.	Unclassified.	70	NA

Form DOT F 1700.7 (8-72) **Reproduction of completed page authorized**

TABLE OF CONTENTS

LIST OF FIGURES

LIST OF TABLES

ACKNOWLEDGMENTS

The authors would like to thank the Iowa Department of Transportation (DOT) and the Iowa Highway Research Board (IHRB) for sponsoring this research. The authors would also like to thank Boone County Engineer Scott Kruse and the management and staff of the Central Iowa Expo for their cooperation and assistance.

EXECUTIVE SUMMARY

Approximately 4.8 miles of roadways at the Central Iowa Expo facility in Boone, Iowa, were reconstructed in 2012 as part of Iowa Highway Research Board (IHRB) project TR-671. The project contained three phases encompassing construction and field testing during freezing and thawing periods to assess the performance of several different pavement foundation technologies for both hot-mix asphalt (HMA) and portland cement concrete (PCC) pavements. The reconstructed roadways have now been in service for more than 10 years, and the Iowa Department of Transportation (DOT) is interested in a Phase IV project to assess the long-term performance of the various pavement system types and construction methods.

This report provides recommendations for two experimental test plan alternatives to assess the long-term performance of the Central Iowa Expo pavement sections. The first plan involves a minimum recommended scope, while the second plan involves a comprehensive scope to more precisely quantify differences between the test sections. A statistical analysis of the data from Phases I through III is detailed, and recommendations based on this analysis are provided regarding the specific sections to test as well as the number and type of tests to perform in each fall and spring thaw season over a period of two years.

The proposed Phase IV evaluation project contains the following objectives:

Objective 1: Evaluate the performance of the pavement foundation sections in terms of stress-dependent in situ resilient modulus and deformation using accelerated cyclic automated plate load testing (APLT).

APLT is an accelerated pavement testing technique that can simulate cyclic vehicle loading conditions expected during the service life of a pavement system to evaluate its time-dependent performance. To meet Objective 1, APLT tests will be performed to measure the in situ resilient modulus M_r values and modulus of subgrade reaction k-values of the foundation layers as well as the stress- and frequency-dependent dynamic modulus values of the asphalt layers. These field tests will generate typical foundation input parameter values that can be used for future Iowa DOT pavement designs.

Objective 2: Analyze the performance and cost of different stabilization techniques.

Based on the performance data to be collected in the proposed phase, along with the material and installation cost data from Phase I, a performance and cost matrix of different stabilization techniques will be developed to help the Iowa DOT strategize pavement foundation design based on project budget and expected performance.

Objective 3: Calibrate frost-depth penetration models in Iowa.

Data from the thermocouples installed on site beneath the pavement layers will be collected and analyzed to further calibrate frost-depth penetration models for the soil and climate conditions of Iowa.

The selected test sections and proposed numbers of tests for each section can be found in Table 4 for the minimum scope and Table 5 for the comprehensive scope of proposed work. In addition to the APLT tests, core hole permeability (CHP) tests and dynamic cone penetrometer (DCP) tests are proposed on a few selected test sections to provide additional engineering measurement values and parameters for pavement design. Additional samples as necessary will be obtained and tested to determine gradation parameters. These parameters will be used in empirical correlations to model seasonal variations in resilient modulus values as part of the Enhanced Integrated Climatic Model (EICM) implemented in AASHTOWare Pavement ME Design.

The Phase IV performance evaluation testing program presented herein considers the previously measured variability (1) within each test section, (2) between the test sections, and (3) between tests performed in each season. The resulting performance data were used to select the minimum number of tests for each section. The testing program was developed with the overall goal of *direct* measurement of not only the in situ mechanistic input parameters necessary for AASHTOWare Pavement ME Design but also the impacts of seasonal variations in the measurement values.

INTRODUCTION

The roadways at the Central Iowa Expo facility located in Boone, Iowa, were reconstructed in 2012 to research the performance of pavement foundations that were engineered and constructed using a variety of new technologies at that time. About 4.8 miles of roadways were paved in segments with either hot-mix asphalt (HMA) or portland cement concrete (PCC). Iowa Highway Research Board (IHRB) project TR-671 was conducted, resulting in three phases and reports by White et al. (2018). The three phases were organized as follows:

- Phase I: Pavement foundation layer construction, May–July 2012
- Phase II: Construction of the pavement layers, June–July 2013
- Phase III: Performance monitoring of the pavement systems, fall 2013 to fall 2016

Within the Expo site, 16 test sections were constructed during Phase I using several pavement foundation stabilization techniques (e.g., cement stabilization, geogrid, compaction). In situ and laboratory tests were performed during construction (in July 2012), then again about three months after construction (in October 2012), then again seven months after construction (in January 2012) during frozen conditions, and finally about nine to ten months after construction (in April/May 2013) during the spring thaw season.

During Phase II, asphalt compaction was monitored using intelligent compaction (IC) technology along with additional in situ point testing.

For Phase III, falling weight deflectometer (FWD) tests and ground penetrating radar (GPR) tests were performed to evaluate the stiffness of the pavement and supporting layers as well as the thickness of the asphalt layer and moisture conditions of the base layer. Additionally, earth pressure cells (EPCs) were installed in the foundation layers at different depths to monitor ground stresses at shallow depths. Thermocouples were installed in two pavement sections and connected to data acquisition systems for long-term motoring. Temperature data were monitored, and the data were collected before winter freezing and after spring thawing. Appendix A provides a list of the many engineering publications resulting from this project.

Now that more than 10 years have passed since the original construction, the Iowa Department of Transportation (DOT) is interested in a reassessment of the various roadways. This report provides recommendations for the experimental test plan. The following are the main objectives of the proposed Phase IV evaluation:

Objective 1: Evaluate the performance of the pavement foundation sections in terms of stress-dependent in situ resilient modulus and deformation using accelerated cyclic plate load testing.

One of the new technologies not available at the time of construction is the automated plate load test (APLT) system. Over the past three years, the Iowa DOT has utilized APLT for direct measurement of resilient modulus and modulus of subgrade reaction values in efforts to develop typical pavement design input parameters (White et al. 2019a, White et al. 2019b).

- APLT tests will be performed to measure the in situ resilient modulus M_r values and modulus of subgrade reaction *k*-values of the foundation layers as well as the stress- and frequency-dependent dynamic modulus values of the asphalt layers. The results will generate typical foundation input parameter values that can be used in future pavement design by the Iowa DOT.
- APLT is an accelerated pavement testing technique that can conduct cyclic loadings to simulate vehicle loading conditions expected during the service life of a pavement system. Therefore, the time-dependent pavement performance can be evaluated.
- The APLT tests will be performed during the spring thaw and fall seasons over a period of two years. Based on the comprehensive field measurements obtained in this phase, comparisons can be made regarding the performance of the different foundation stabilization techniques to rank the best performing systems versus the less well performing systems.

Objective 2: Analyze the performance and cost of different stabilization techniques.

The material and installation costs for the 16 test sections were collected during Phase I of the project. Based on the performance data to be collected in the proposed phase, a performance and cost matrix of different stabilization techniques will be developed. This will help the Iowa DOT strategize pavement foundation design based on project budget and expected performance.

Objective 3: Calibrate frost-depth penetration models in Iowa.

Data from the thermocouples installed on site beneath the pavement layers will be collected and analyzed to calibrate frost-depth penetration models for the soil and climate conditions of Iowa.

In this report, a detailed testing plan is outlined along with a list of test sections to be evaluated, the type of tests to be performed, and the associated mechanistic measurements. The experimental plan is organized into minimum and comprehensive test plan alternatives, where the minimum plan contains the minimum recommended tests and the comprehensive plan contains additional beneficial tests to more precisely verify small differences between sections. The IHRB is presented with the option of the minimum or comprehensive plan pending availability of funding.

BACKGROUND

Summary of Test Results and Findings from Phases I through III

Test Sections and As-Built Profiles

The project site consists of 13 roads oriented in the north-south direction (denoted as 1st St. to 13th St.) and 3 roads oriented in the east-west direction (denoted as South Ave., Central Ave., and North Ave.). Aerial imagery of the Expo site is shown in Figure 1 and Figure 2. All roads were reconstructed except 13th St., which was paved with HMA earlier in 2012.

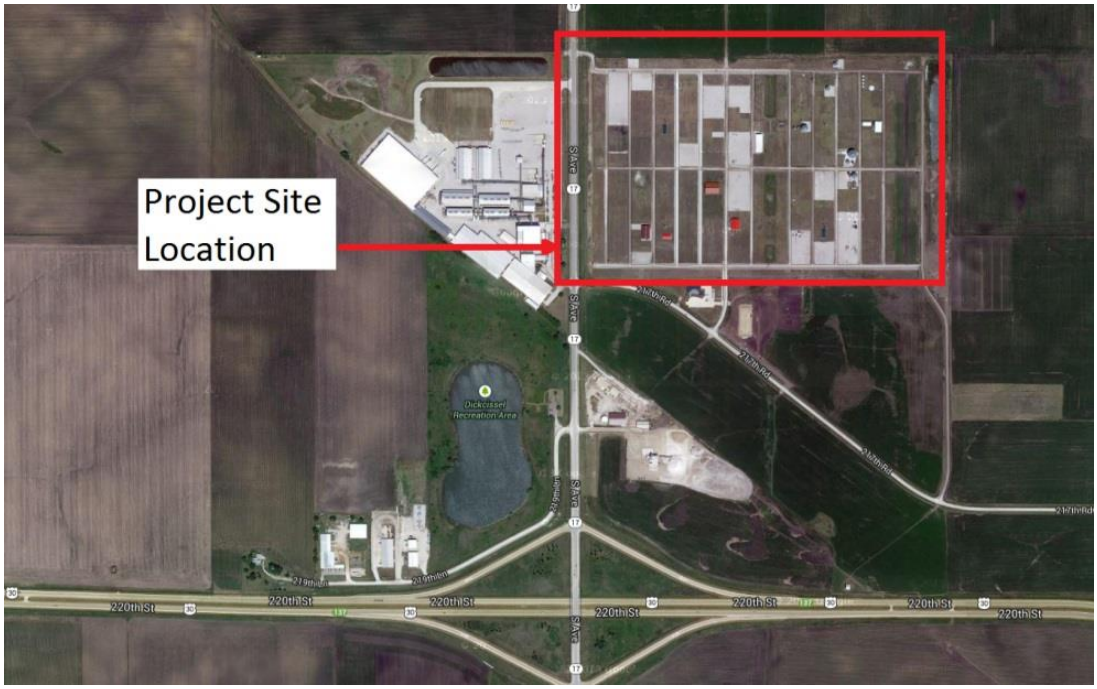

White et al. 2018

Figure 1. Aerial imagery of Expo site in Boone County, Iowa

White et al. 2018

Figure 2. North-south and east-west road layout at the Expo site (aerial image from June 2012)

As summarized in Table 1, 16 test sections were constructed on the north-south roads that incorporated the following pavement foundation layer stabilization methods (Figure 3):

- Woven and nonwoven geotextile at subgrade/subbase interface
- Triaxial and biaxial geogrid at subgrade/subbase interface
- 4 in. and 6 in. geocells in subbase layer + nonwoven geosynthetics at subgrade/subbase interface
- Portland cement (PC) stabilization of subgrade
- Fly ash (FA) stabilization of subgrade
- PC stabilization of recycled subbase (reclaimed from existing granular subbase layer on site)
- PC + fiber stabilization of recycled subbase with white polypropylene (PP) fibers
- PC + fiber stabilization of reclaimed subbase with black monofilament PP (MF-PP) fibers
- Mechanical stabilization (by mixing subgrade with reclaimed subbase)
- Reclaimed subbase between modified subbase (MSB) and subgrade
- High-energy impact compaction of subgrade

Table 1. Summary of foundation layer profiles for all test sections

Street	Section	Station	Foundation Layer Profile[a] (above existing/natural subgrade)	
1st St.	North	107+14.00 to 113+88.00	6 in. (5.5 in. actual) MSB[b]	12 in. compacted subgrade[c]
	South	100+12.00 to 106+86.00		
2nd St.	North	207+14.00 to 213+88.00	6 in. (6.1 in. actual) MSB[b]	12 in. mechanically stabilized subgrade
	South	200+12.00 to 206+86.00		
3rd St.	North	307+14.00 to 313+88.00	2 in. MSB[b]	4 in. geocell reinforced MSB, NW geotextile
	South	300+12.00 to 306+04.00	1 in. MSB[b]	6 in. geocell reinforced MSB, NW geotextile
	South	306+04.00 to 306+86.00		6 in. geocell reinforced MSB (no geotextile)
4th St.	North	407+14.00 to 413+88.00	6 in. (7.0 in. actual) MSB[b]	NW geotextile
	South	400+12.00 to 406+86.00		woven geotextile
5th St.	North	507+14.00 to 513+88.00	6 in. (6.1 in. actual) MSB[b]	triaxial geogrid
	South	500+12.00 to 506+86.00	6 in. (5.8 in. actual) MSB[b]	biaxial geogrid
6th St.	North	4026+93.49 to 4032.85.49	6 in. (4.5 to 5 in. actual) MSB[b]	6 in. reclaimed subbase + 5% (5.6% actual) PC + 0.4% (0.5% actual) PP fibers
		4032+85.49 to 4033+67.49		6 in. reclaimed subbase + 0.4% (0.5% actual) PP fibers
	South	4020+82.30 to 4026+65.49	6 in. (4.5 to 5 in. actual) MSB[b]	6 in. reclaimed subbase + 5% (5.5% actual) PC + 0.4% (0.5% actual) MF-PP fibers
		4020+21.30 to 4020+82.30		6 in. reclaimed subbase + 0.4% (0.4% actual) MF-PP fibers
7th St.	North	707+14.00 to 713+88.00	6 in. (5.5 in. actual) MSB[b]	6 in. reclaimed subbase + 5% (6.2% actual) PC
	South	700+12.00 to 706+86.00		6 in. reclaimed subbase + 5% (5.2% actual) PC
8th St.	North	807+14.00 to 813+88.00	6 in. (6.0 in. actual) MSB[b]	Compacted subgrade[d]
	South	800+12.00 to 806+86.00		
9th St.	North	907+14.00 to 913+88.00	6 in. (6.0 in. actual) MSB[b]	6 in. reclaimed subbase
	South	900+12.00 to 906+86.00		
10th St.	North	1007+14.00 to 1013+88.00	6 in. (5.5 in. actual) MSB[b]	12 in. compacted subgrade[c]
	South	1000+12.00 to 1006+86.00		—
11th St.	North	1107+14.00 to 1113+88.00	6 in. (6.0 in. actual) MSB[b]	12 in. 10% (11.4% actual) PC stabilized subgrade
	South	1100+12.00 to 1106+86.00		12 in. 20% (22.3% actual) Port Neal FA stabilized subgrade
12th St.	North	1207+14.00 to 1213+88.00	6 in. (6.0 in. actual) MSB[b]	12 in. 15% (15.8% actual) Ames FA stabilized subgrade
	South	1200+12.00 to 1204+46.00	6 in. (5.7 in. actual) MSB[b]	12 in. 10% (10% actual) Port Neal FA stabilized subgrade
	South	1204+46.00 to 1206+86.00	6 in. (6.0 in. actual) MSB[b]	12 in. 10% (10% actual) Muscatine FA stabilized subgrade
North Ave.	West[e]	3000+02.50 to 3002+02.50	9 in. MSB[f]	6 in. reclaimed subbase, biaxial geogrid
	West[e]	3002+02.50 to 3004+02.50		6 in. reclaimed subbase, triaxial geogrid
	East[e]	3004+02.50 to 3023+38.14		6 in. reclaimed subbase
South Ave.	West[e]	1001+00.00 to 1003+00.00	9 in. MSB[f]	6 in. reclaimed subbase, biaxial geogrid
		1003+00.00 to 1005+00.00		6 in. reclaimed subbase, biaxial geogrid
		1005+00.00 to 1009+06.08		6 in. reclaimed subbase
South Ave.	East[e]	1009+94.00 to 1011+94.00	9 in. MSB[f]	6 in. reclaimed subbase, biaxial geogrid
		1011+94.00 to 1013+94.00		6 in. reclaimed subbase, biaxial geogrid
		1013+94.00 to 1023+39.91		6 in. reclaimed subbase
Central Ave.	East/West	2000+01.43 to 2023+39.59	9 in. MSB[f]	6 in. reclaimed subbase

Source: White et al. 2018

[a] Thicknesses provided are nominal unless indicated as actual in parenthesis (actual measurements were obtained from test pits); [b] Crushed limestone; [c] Existing subgrade scarified, moisture conditioned, and compacted; [d] The original subbase layer topped with chip seal was compacted with high-energy impact roller and the subbase layer was excavated down to about 6 in. below final grade and replaced with MSB; [e] With reference to 6th St.; [f] Mixture of recycled PCC and asphalt

Mechanical stabilization

High-energy impact compaction

6 in. geocell over woven geosynthetic layer placed on subgrade

Woven geotextile over subgrade

Nonwoven geotextile over subgrade

Triaxial geogrid placed over subgrade

Biaxial geogrid over subgrade

PC + White PP Fiber stabilization of reclaimed subbase

PC + Black MF-PP fiber stabilization of reclaimed subbase

PC stabilization of reclaimed subbase

PC stabilization of subgrade

FA stabilization of subgrade

Figure 3. Different stabilization methods utilized at the Expo site during construction in July 2012

Construction of the sections required removing the existing deteriorated chip seal surface and subbase and 6 to 12 in. of subgrade. The subgrade consisted primarily of wet soils classified as

lean clay (CL) or A-6(5). Groundwater was at depths of 3 to 6 ft below the original grade across the site and at depths of about 12 ft or greater near drainage features.

All north-south test sections except one were topped with a nominal 6 in. of MSB material classified as GP-GM or A-1-a (7% fines content), whereas the 6 in. geocell section required 7 in. of MSB. All east-west test sections were topped with a nominal 9 in. of MSB material. Crushed limestone was used in the MSB layer on all north-south roads, and a mixture of recycled concrete and recycled asphalt was used in the MSB layer on all east-west roads. Six north-south test sections (6th St., 7th St., and 9th St.) and the east-west test sections consisted of 6 in. of recycled subbase material classified as SM or A-1-a (14% fines content) between the subbase and subgrade layers.

Phase I In Situ Test Results and Key Findings

Details of construction and results from in situ testing during construction are provided in White et al. (2018). A color-coded map of intelligent compaction measurement values from a vibratory smooth drum roller used during foundation layer construction is shown in Figure 4. The map enables a visual assessment of the spatial variability of the foundation layer support conditions across the site.

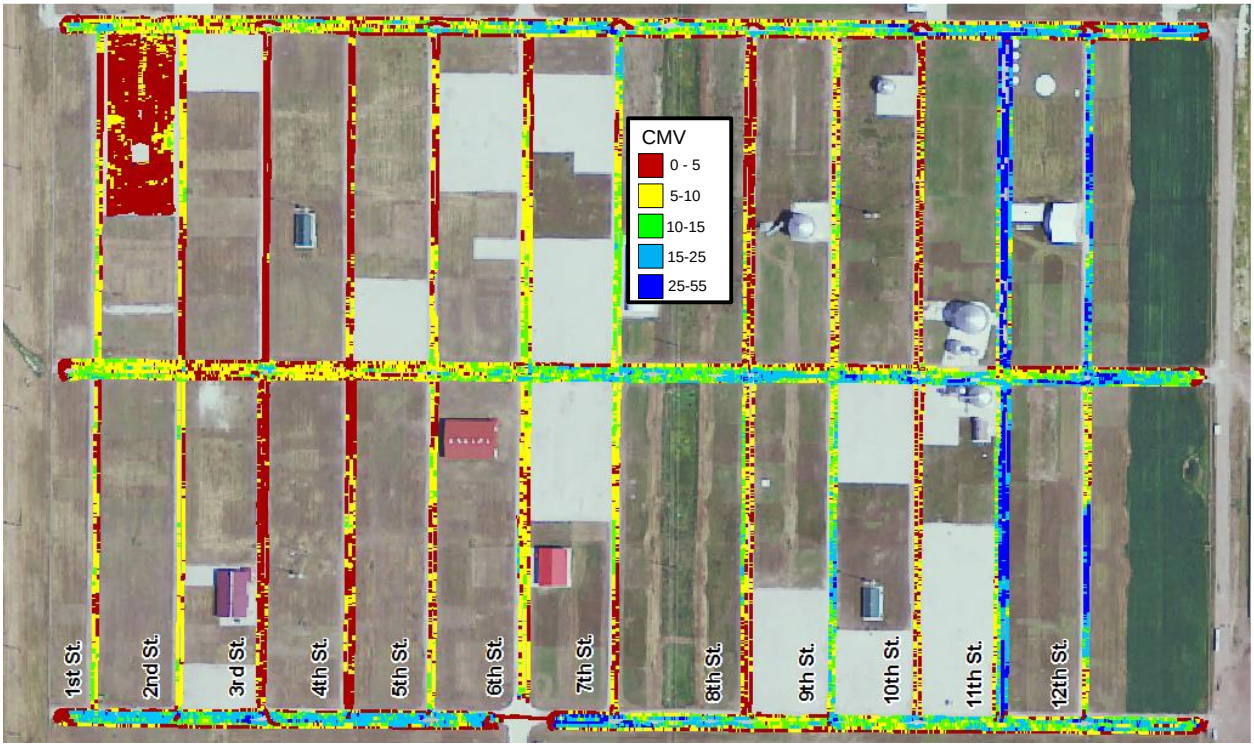

White et al. 2018

Figure 4. Compaction meter value (CMV) map measured using CS683 intelligent compaction roller from July 2012

Some of the key findings from the Phase I testing during and shortly after construction of the test sections, as they relate to future performance monitoring, are as follows:

- Intelligent compaction measurement values provided near-continuous digital records of index values, which were correlated to ground stiffness and showed variations between the test sections as well as locations of lower-stiffness materials within sections.

- FWD composite elastic moduli values from each test section after construction in July 2012 (i.e., never-frozen) ranged from 5.4 to 44.5 ksi (Figure 5). Test sections with PC-stabilized subgrade, FA-stabilized subgrade, or PC-stabilized reclaimed gravel subbase produced the highest moduli values. Test sections with mechanically stabilized subgrade, compacted subgrade, or untreated reclaimed gravel subbase produced comparatively higher moduli values than the control test sections, which had no subgrade compaction or other treatment.

- Average FWD composite elastic moduli during April 2013 (i.e., thaw-weakened) ranged from 1.6 to 23.1 ksi (Figure 6 and Table 2). All test sections experienced reductions in moduli values as conditions transitioned from never-frozen to thaw-weakened (by about 2 to 9 times on average). Test sections with PC-stabilized subgrade or PC-stabilized reclaimed gravel subbase produced the highest moduli values.

- Correlations between thaw-weakened and never-frozen elastic moduli values suggested that PC-stabilized pavement foundations are less susceptible to thaw weakening than untreated pavement foundations or FA-stabilized pavement foundations.

- Laboratory freeze-thaw durability tests showed that subgrades stabilized with fly ash exhibited improvements, including decreasing levels of frost-heave and thaw-weakening susceptibility, as fly ash content increased up to 15%. Greater improvement was observed to result from a shorter fly ash set time. Subgrades and subbases stabilized with cement showed low to negligible frost susceptibility. For subbases, the addition of fibers increased the pre-test and post-test (saturated) California bearing ratio (CBR) values slightly. Comparatively, the addition of cement reduced the heave rates and increased the CBR values significantly. Results also indicated that curing time and compaction delay time influence the freeze-thaw performance of chemically stabilized soils.

- Shortly after construction and after spring thaw, mechanically stabilized test sections that had undergone in situ mixing of recycled aggregate with the existing subgrade (2nd St.) and over-excavation and replacement (9th St.) produced comparatively higher elastic moduli values than the control section (10th St.), which had no subgrade modification. There was no statistical evidence to suggest that over-excavation and replacement of the existing pavement foundation yielded better performance than mechanical stabilization of the pavement foundation, or vice versa, shortly after construction. However, after spring thaw, results showed that the section with over-excavation and replacement (9th St.) performed better than the section with mechanical stabilization (2nd St.).

- Laboratory freeze-thaw testing showed that the mechanically stabilized subgrade used in this study exhibited strength and stiffness behavior similar to that of the on-site recycled material at optimum environmental conditions. During thaw-weakening conditions, the mechanically stabilized subgrade exhibited strength and stiffness behavior like that of the native subgrade.

- Elastic moduli values determined via FWD in never-frozen conditions showed statistically significant relationships with both subbase and subgrade layer penetration index values from dynamic cone penetrometer (DCP) tests at that time. However, FWD elastic moduli values after thawing showed a strong correlation with the subgrade penetration index but not with the subbase layer penetration index at that time. This emphasizes the importance of subgrade support for the composite response on top of the subbase layer.

- Field air permeameter tests were conducted to rapidly determine the field saturated hydraulic conductivity of the modified subbase layer (Figure 7). Testing was focused on three test sections (5th St. South, 8th St. South, and 11th St. South). Degradation was observed in the modified subbase layer; however, the level of degradation varied between sections (Figure 8). The section with the highest support values (i.e., high CBR and elastic moduli values) with PC-stabilized subgrade (11th St. South) showed the highest amount of degradation of the aggregate subbase and the lowest hydraulic conductivity. The control section (with only granular subbase over uncompacted subgrade on 8th St.) yielded the lowest support values but the highest hydraulic conductivity. The geogrid-reinforced aggregate section (5th St. South) provided comparatively better support conditions than the control section and intermediate hydraulic conductivity values.

- Traditional nuclear gauge density testing was also performed. The results revealed that this approach to quality assessment has critical shortcomings, including lack of reproducibility, infrequent testing, and failure to capture the wide range in stiffness values.

- Figure 9 summarizes the combined material and installation costs for the test sections constructed for this project. The cost data were compiled from all six contractor bidders' unit prices as requested in the plans and specifications. Geosynthetics are at the low end of the cost range, chemical stabilization is at the intermediate range, and special products (fibers and geocell) are at the high end of the range. The quantities used on this project ranged from about 140 m^2 to 420 m^2.

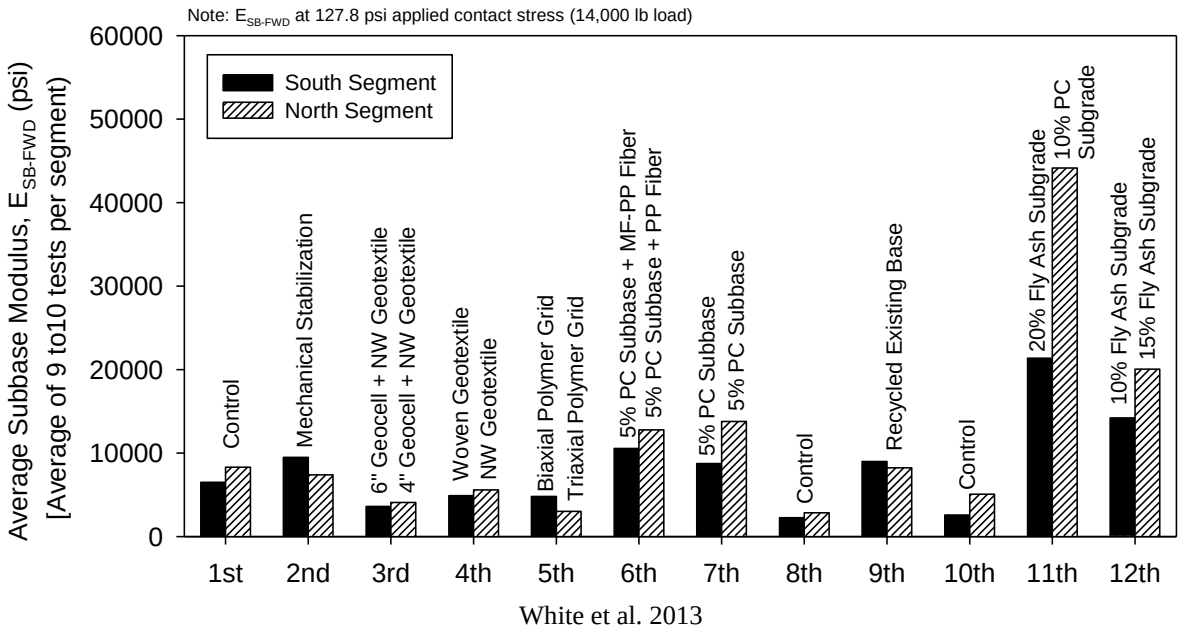

Figure 5. Average composite elastic modulus measurements from FWD tests conducted on the subbase layer after construction in July 2012

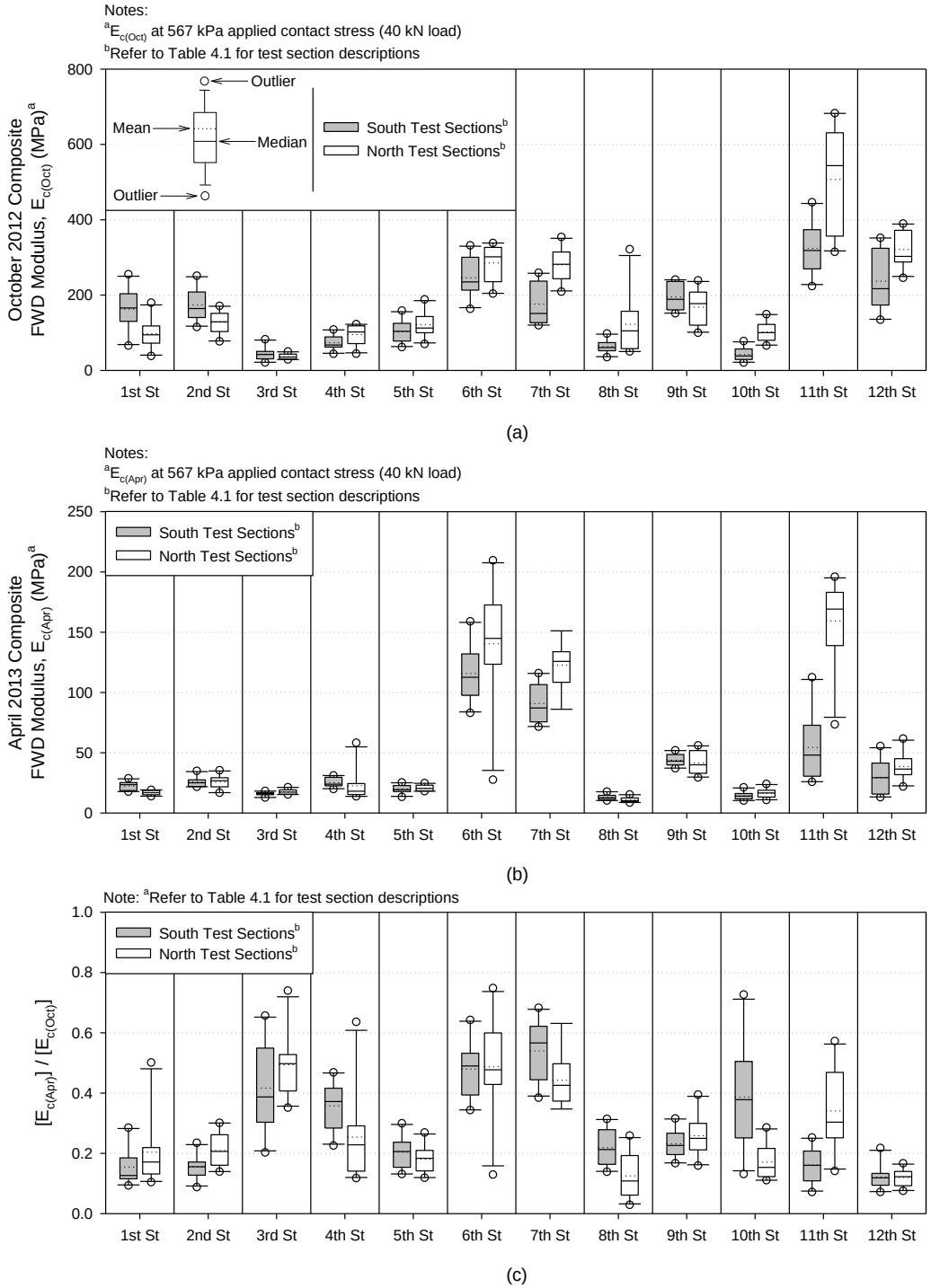

White et al. 2018
Note: To convert MPa to psi, multiply by 145.038.

Figure 6. FWD test results from October 2012 (never frozen) versus April 2013 (spring thaw): (a) composite moduli from October 2012, (b) composite moduli from April 2013, and (c) ratios of October 2012 to April 2013 FWD composite moduli

Table 2. Summary statistics of elastic modulus values determined from FWD testing in October 2012 versus April 2013 (after spring thaw)

Street		October 2012 Average Composite FWD Modulus, $E_{c(Oct)}$ (MPa) [COV[a] (%)]	April 2013 Average Composite FWD Modulus, $E_{c(Apr)}$ (MPa) [COV[a] (%)]	$E_{c(Apr)}$ / $E_{c(Oct)}$ [COV[a] (%)]
1st	South	163 [34]	22 [17]	0.15 [42]
	North	98 [39]	17 [11]	0.20 [57]
2nd	South	174 [24]	26 [16]	0.16 [25]
	North	128 [24]	26 [22]	0.21 [28]
3rd	South	44 [42]	16 [10]	0.42 [36]
	North	37 [19]	18 [12]	0.49 [21]
4th	South	74 [27]	25 [15]	0.36 [22]
	North	95 [28]	23 [58]	0.25 [60]
5th	South	103 [29]	20 [17]	0.20 [26]
	North	122 [28]	21 [12]	0.18 [26]
6th	South	246 [21]	116 [21]	0.48 [20]
	North	285 [17]	140 [35]	0.49 [34]
7th	South	176 [32]	91 [18]	0.54 [18]
	North	280 [16]	123 [16]	0.44 [20]
8th	South	63 [28]	13 [19]	0.22 [29]
	North	123 [66]	11 [19]	0.13 [59]
9th	South	195 [18]	44 [11]	0.23 [21]
	North	168 [29]	41 [23]	0.26 [27]
10th	South	43 [41]	14 [23]	0.39 [45]
	North	103 [27]	17 [23]	0.17 [35]
11th	South	324 [21]	54 [54]	0.16 [36]
	North	507 [28]	159 [23]	0.34 [39]
12th	South	237 [33]	29 [48]	0.12 [33]
	North	321 [15]	39 [29]	0.12 [23]

[a] COV = coefficient of variation
Multiply by 145.038 to convert MPa to psi

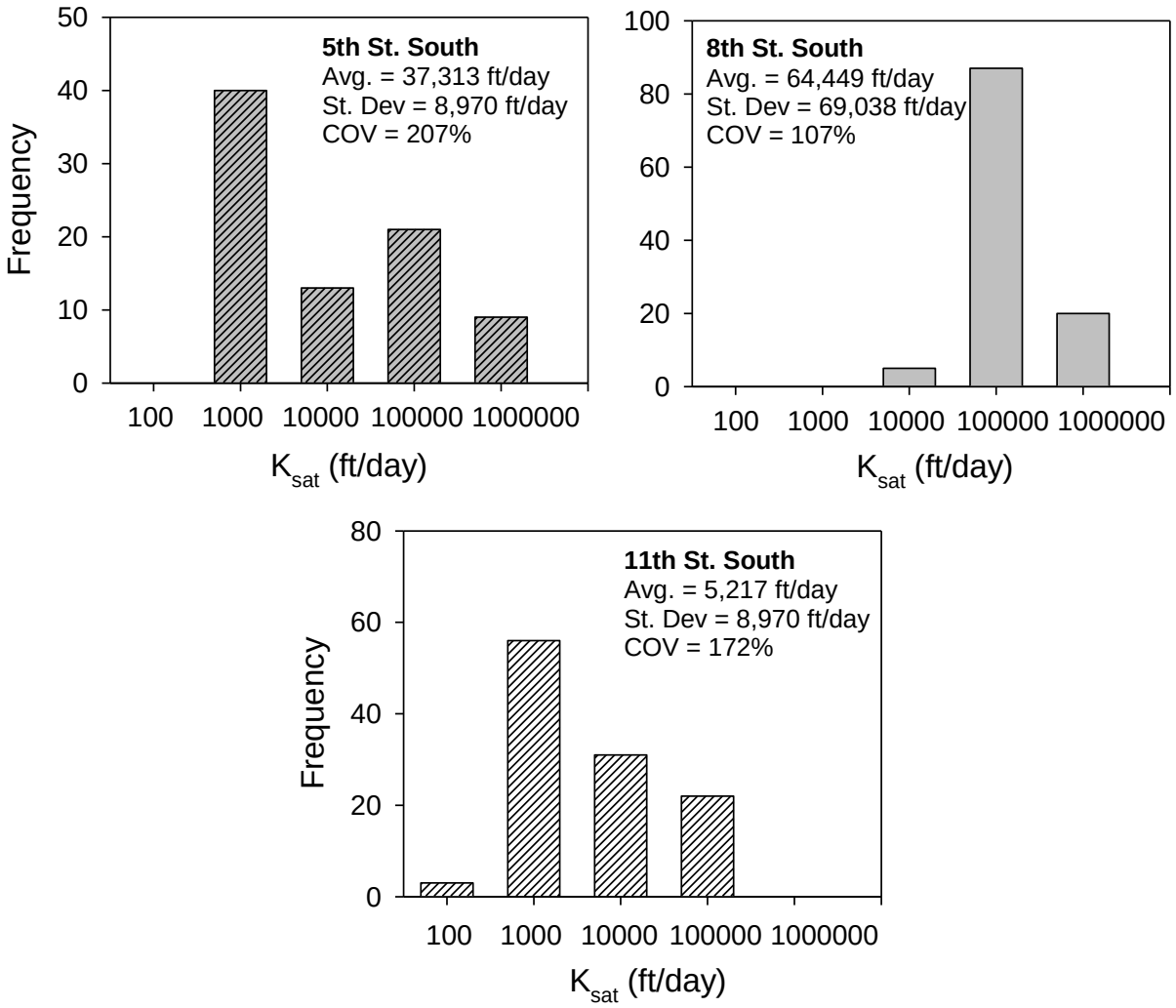

White et al. 2018

Figure 7. Histograms of saturated hydraulic conductivity (K_{sat}) measurements on the modified subbase layer on three test sections after construction in July 2012

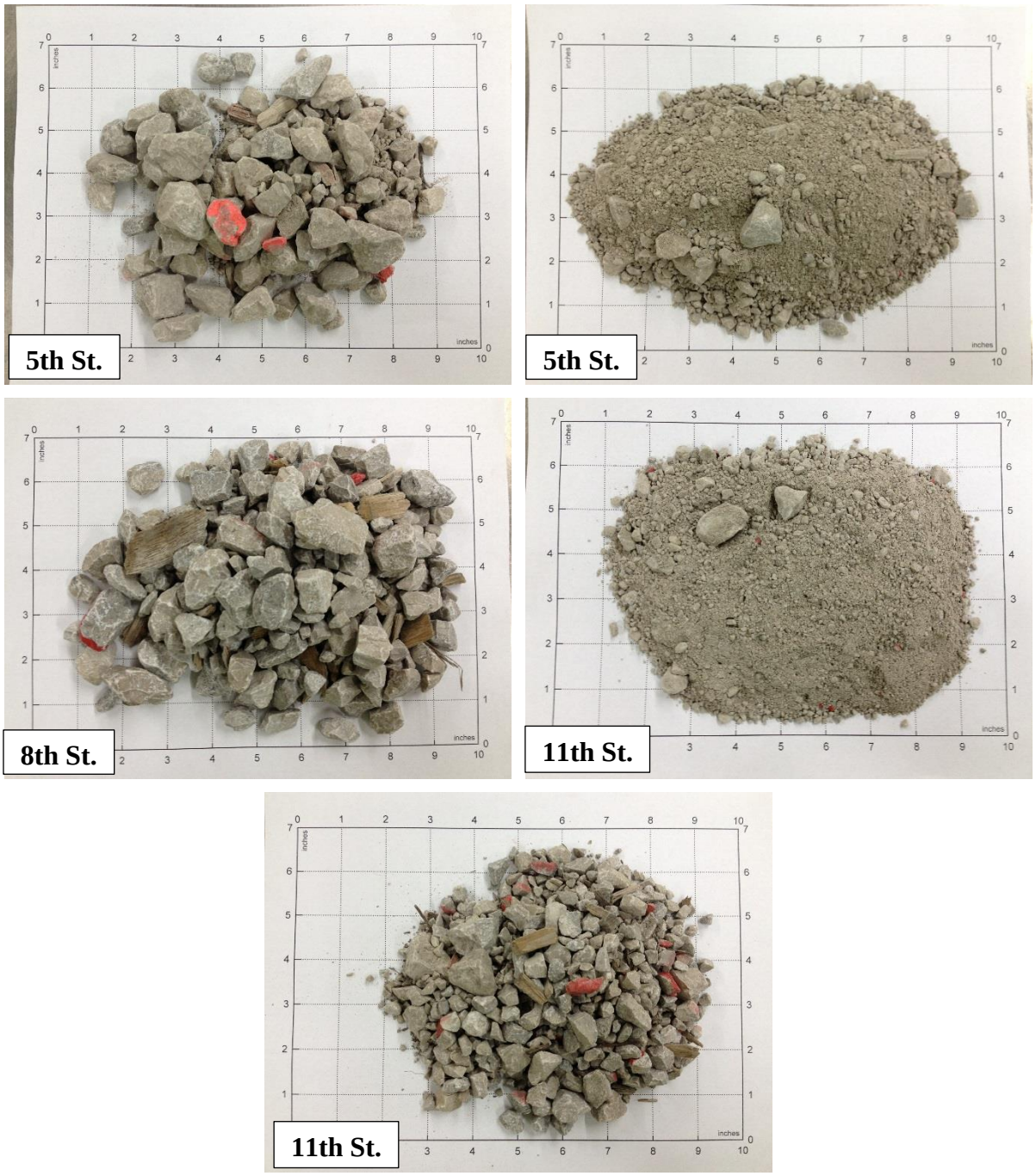

Figure 8. Modified subbase samples collected from the three test sections after construction (July 2012)

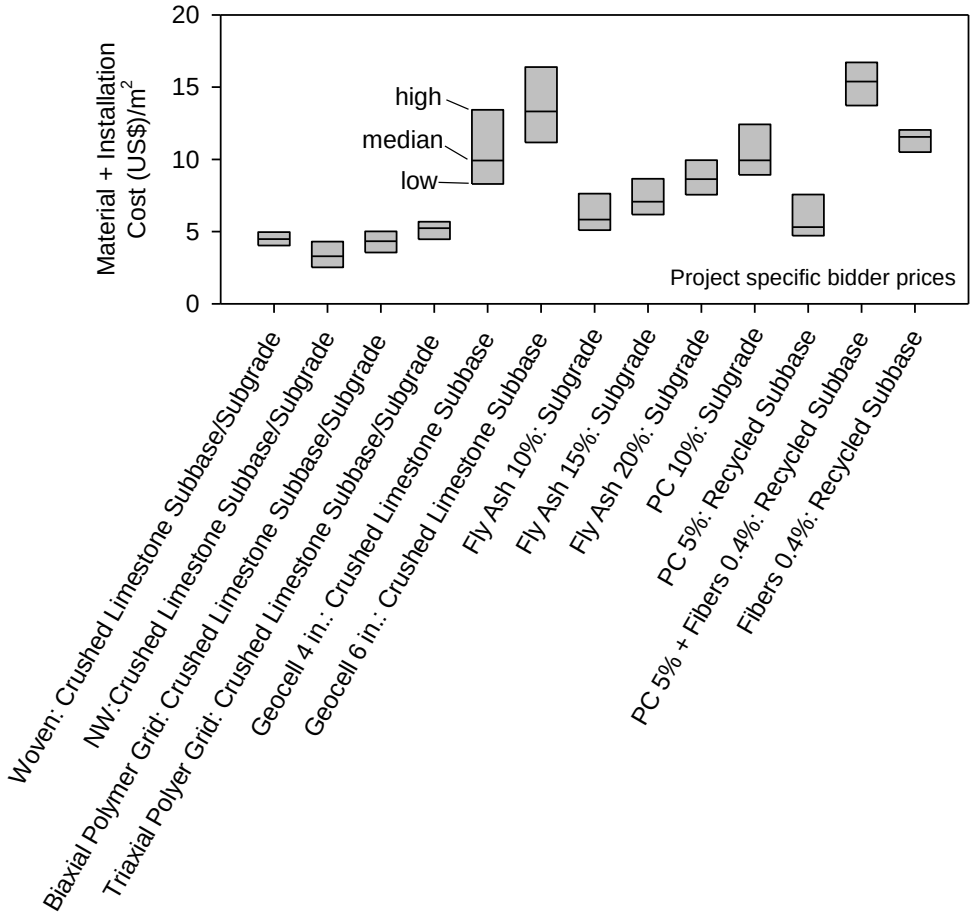

Figure 9. Bid prices for stabilization material and placement based on six bidders

Phases II and III In Situ Test Results and Key Findings

Pavement layer construction occurred in June and July 2013. All test sections oriented in the north-south direction, except those on 6th street, were paved with a nominal 4 in. asphalt base course layer and a nominal 2 in. asphalt surface course layer. The 6th street north-south sections and all east-west roadways were paved with 6 in. of PCC. A geosynthetic composite drainage layer was installed directly beneath the PCC layer in the 6th St. South section for comparison of drainage with the 6th St. North section, which did not have a geocomposite layer. A geocomposite layer was also installed on the 11th St. North section (stabilized with PC in the subgrade) directly beneath the asphalt layer, and a control section without a geocomposite layer was constructed for comparison of drainage performance between the two sections.

All test sections were mapped with a Hamm roller to measure Hamm measurement values (HMVs) prior to paving. These values were compared with measurements obtained on the asphalt base and surface course layers to assess the significance of support layer conditions on the surface layer compaction properties. Asphalt density was monitored with a nuclear gauge at multiple compaction passes and was correlated with the roller measurements.

Shortly after paving was completed, performance monitoring testing was conducted from fall 2013 to fall 2016. This testing included FWD testing on the pavement layer in fall 2013 and after spring thaw in spring 2014 and GPR measurements to evaluate the thickness of the asphalt layer and the moisture conditions of the base layer. In addition, foundation layer temperatures were monitored in one test section with an asphalt surface layer and one test section with a PCC surface layer to a depth of about 5 ft below the ground surface for the duration of the monitoring period (see Figure 10 and Figure 11).

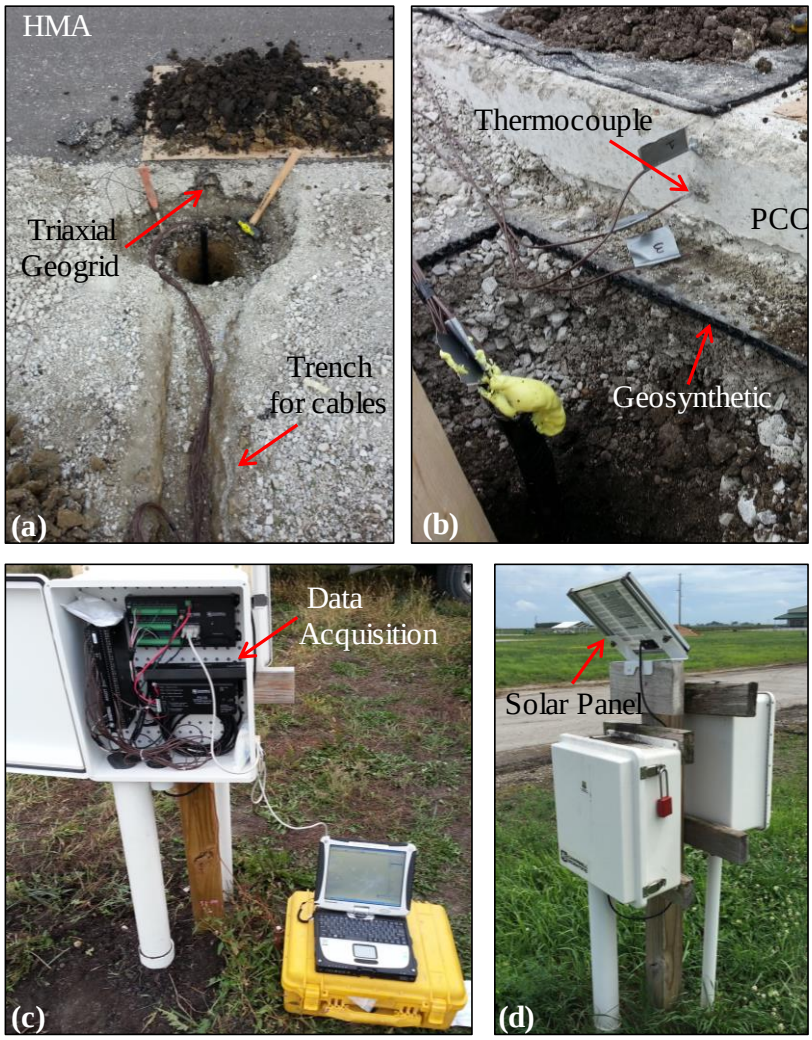

White et al. 2018

Figure 10. Thermocouple installation at the (a) 5th St. Expo 1 and (b) 6th St. Expo 2 sites and (c and d) data acquisition system

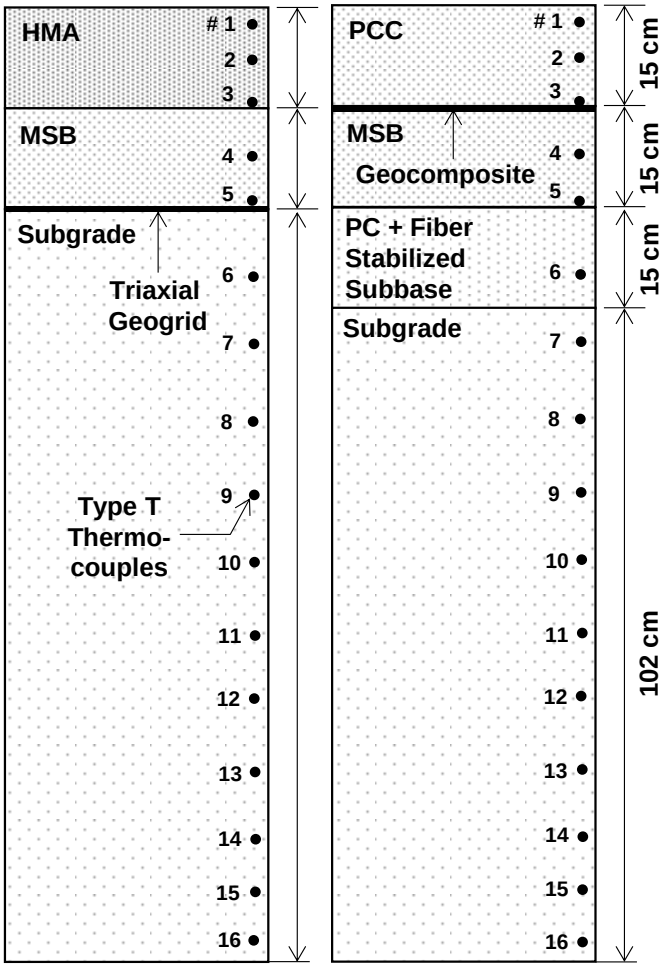

White et al. 2018
Note: To convert cm to inches, multiply by 0.3937.

Figure 11. Pavement profiles with thermocouples at the Expo 1 (left) and Expo 2 (right) sites

Many highway agencies currently use FWD testing as part of routine testing of pavements in situ. Different agencies use different back- or forward-calculation procedures to determine layer moduli values. Many agencies also rely on empirical relationships in determining the design moduli values. The field test results from the previous study were analyzed to assess statistical uncertainties associated with the values determined from the different procedures (AASHTO and Hogg forward-calculation and ERIDA back-calculation) and empirical relationships.

Details of construction and results from in situ testing during pavement layer construction and performance monitoring are provided in White et al. (2018). Some of the key findings from the testing in Phases II and III, as they relate to future performance monitoring, are as follows:

- In general, HMVs during asphalt pavement construction were higher when placing asphalt over stiff pavement foundations. All HMV measurements on the asphalt layers correlated with statistical significance to HMV measurements obtained on the foundation layers.

- For asphalt construction over softer pavement foundations, HMV increased with each additional pavement layer. For asphalt construction over stiff foundations, in general, the pavement foundation HMV was greater than base course HMV, and the base course HMV was less than the surface course HMV.

- Asphalt pavement relative compaction, whether obtained from nuclear density gauge tests or pavement cores, did not correlate with HMV measurements. However, FWD measurements strongly correlated with HMV measurements.

- Comparison of three different forward- and back-calculation procedures for FWD data analysis indicated significant differences in the estimated moduli values for the asphalt, base, and subgrade layers. Standard errors of the estimated values were in the range of 1.9 ksi for the subgrade layers, over 16.8 ksi for the base layers, and over 435 ksi for the asphalt layers.

- Numerous regression relationships have been documented in the literature between DCP test measurements and moduli values. Upper and lower bounds were presented based on the available relationships. The bounds suggest that the predicted moduli values can have an error of ± 7 to 49 ksi if DCP penetration resistance values are between 2 and 10 mm/blow and an error of ± 1.5 to 7 ksi if penetration resistance values are greater than 10 mm/blow.

- The number of freeze-thaw cycles with depth calculated for each year from 2013 to 2016 based on the temperature monitoring data at both Expo sites is presented in Figure 12. The number of freeze-thaw cycles decreased with depth, as expected. The number of freeze-thaw cycles in air was between 41 and 65 and decreased to about 3 to 11 cycles near the bottom of the pavement. Although there were differences between the PCC and HMA layers in the number of freeze-thaw cycles, the numbers of freeze-thaw cycles were similar as depth increased. From the bottom of the MSB layer at a depth of about 40 cm, fewer than 3 cycles were found at both locations. The deepest freeze-thaw cycle during the monitored timeframe was observed between 47 in. and 55 in.

- Connecting these 0ºC points provided the estimated isothermal lines (Figure 13). The upper areas of the isothermal lines were called “frost zones,” which indicated the length of freezing periods at different depths. The lowest point of the isothermal line was the maximum frost penetration of the year. Results showed a relatively large frost zone during the 2013–2014 winter, two separated medium frost zones during the 2014–2015 winter, and a smaller zone for the 2015–2016 winter for each street. In general, differences of < 1 in. to 5 in. were found between the maximum frost penetrations at the two Expo sites.

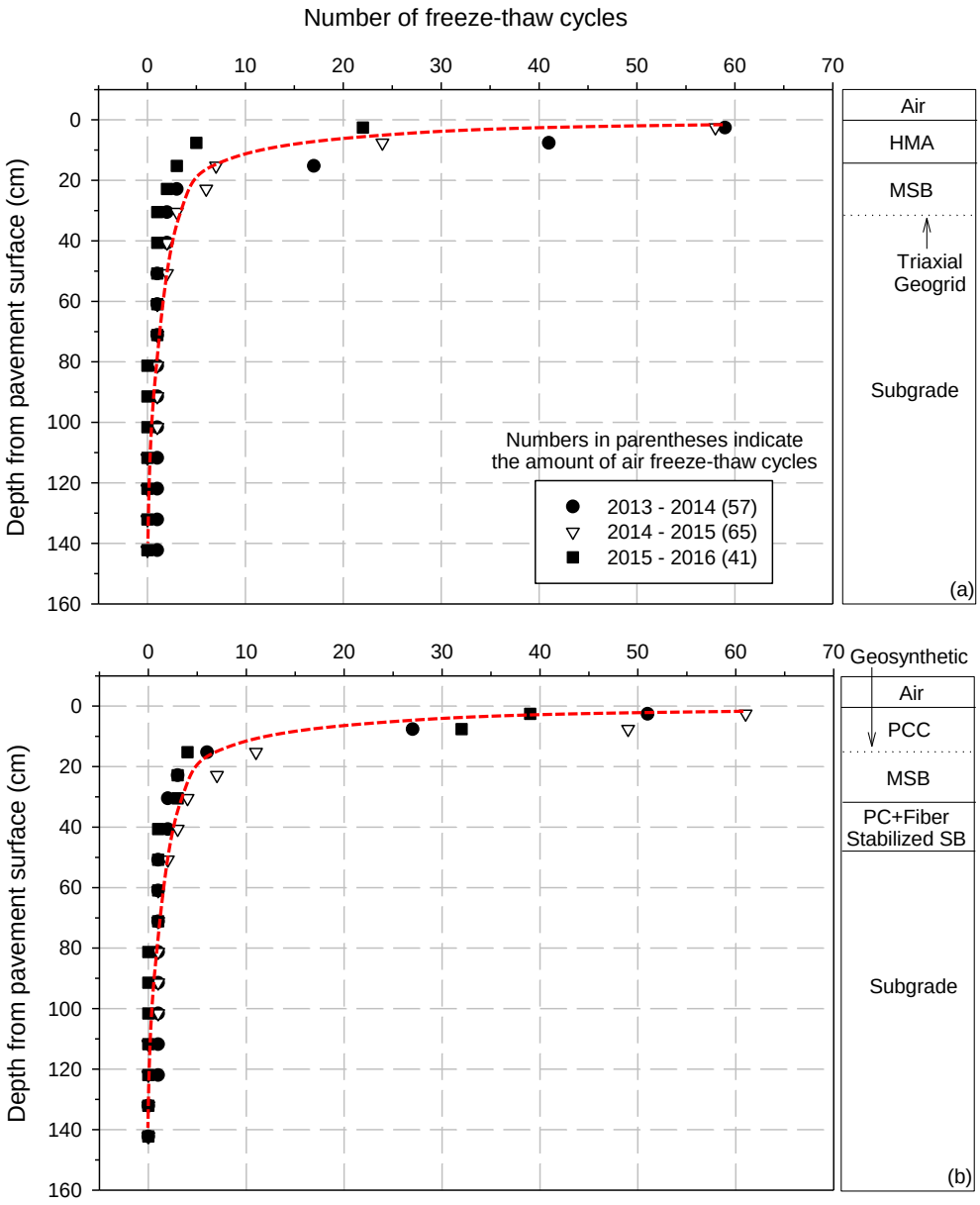

White et al. 2018

Note: To convert cm to inches, multiply by 0.3937.

Figure 12. Freeze-thaw cycles versus depth at the (a) Expo 1 and (b) Expo 2 sites

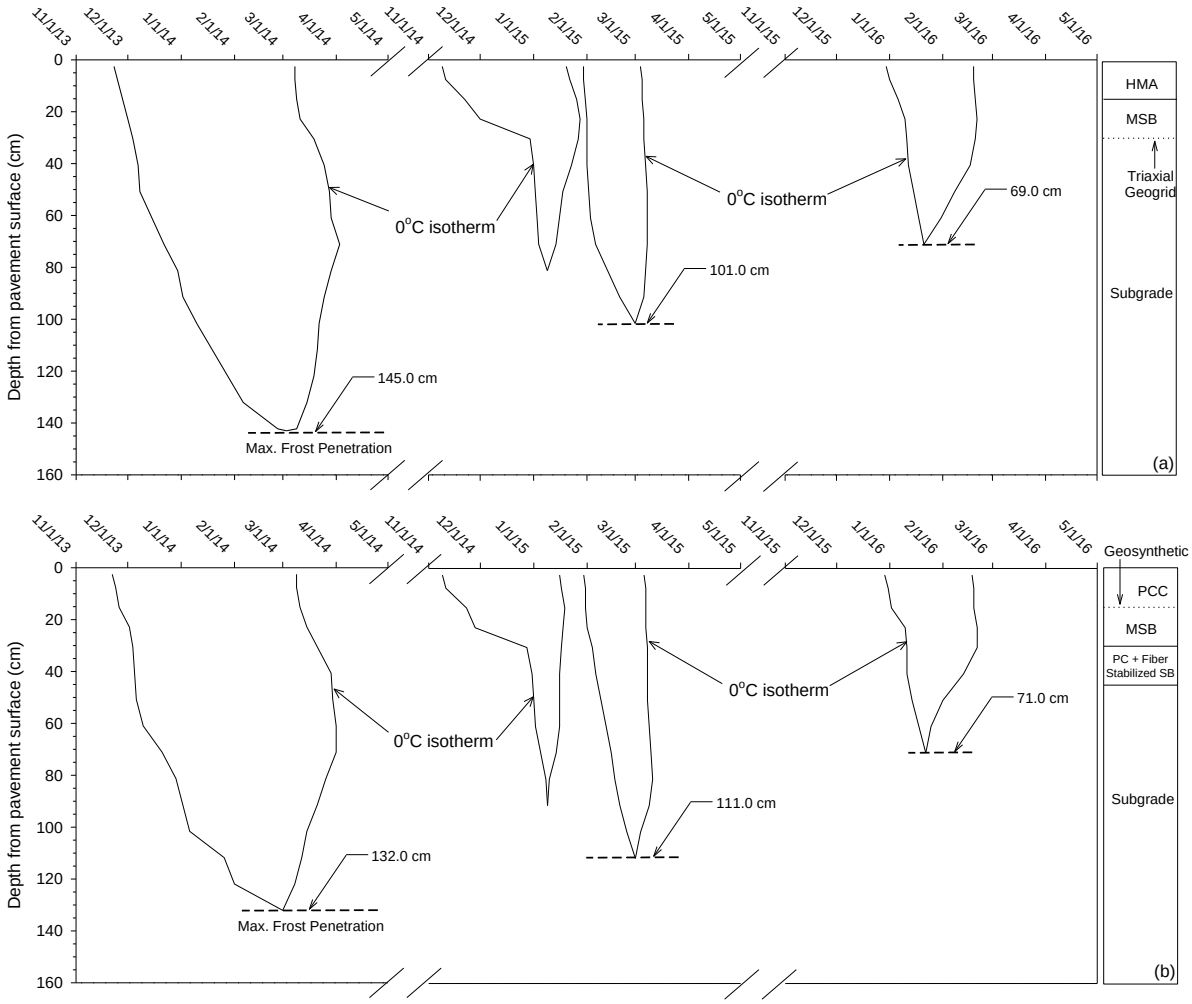

White et al. 2018
Note: To convert cm to inches, multiply by 0.3937.

Figure 13. Frost zones from 2013 to 2016 at the (a) Expo 1 and (b) Expo 2 sites

Lessons Learned, Limitations, and Recommendations from Expo Testing

This project generated significant and important information regarding the mechanistic properties of pavement foundation support for a range of foundation improvement/stabilization methods. The test sections at the Central Iowa Expo facility are unique in terms of the range of technologies used and for the fact that the performance data particularly isolate the influence of seasonal changes without any loading. Some significant lessons learned from this project and the limitations of the findings are identified in White et al. (2018) to identify the path forward for the Iowa DOT in terms of implementing the findings into design and construction practice and future research/testing on these test sections. Key findings are as follows:

- Traditional nuclear gauge moisture-density testing has played an important role in earthwork quality assessment specifications in the United States for decades. This form of quality control/quality assurance (QA/QC) testing can be effective but has shortcomings due to

regulations, test reproducibility, limited test frequency, and the fact that the results only serve as a surrogate to strength and stiffness design requirements. Results showed that all the QC agent test results met the target moisture and density criteria, while the QA agent test results were much more variable on both counts. It was clear that nuclear density testing does not identify wide stiffness variations resulting from different treatments and materials.

- The distinct advantage of the strength/stiffness-related measurements performed in this study was that they identified the variations in support values between different stabilization sections. While these measurements were critical in identifying the relative differences in the strength/stiffness properties between the test sections, they all produced different measurement values that can potentially be used to *estimate* the mechanistic input parameters used in the pavement design process. However, the following limitations of these test measurements must be acknowledged:

    - Thus far, there is no supporting evidence that these measurements can be reliably used to predict the key mechanistic input parameters used in design (i.e., resilient modulus [M_r] and modulus of subgrade reaction [*k*-value]) with high statistical confidence.

    - Empirical relationships have been published between DCP or CBR measurements and M_r and *k*-values, but all of these relationships produce significantly different numbers and therefore present significant uncertainty in selecting an appropriate value in design. Local or regional correlations can be more reliable but can be very time-consuming to generate.

    - In situ M_r is commonly predicted from nondestructive surrogate tests including the FWD or lightweight deflectometer (LWD), but the elastic moduli values calculated from these test devices based on elastic deformations are often confused with resilient modulus values, which are based on resilient (i.e., recoverable) deformations. One of the major limitations of these nondestructive surrogate tests is the lack of a conditioning stage prior to testing. During pavement construction, pavement foundation materials are subjected to relatively high loads from construction traffic and compaction equipment. In response to these loads, aggregate particles rearrange, resulting in higher density and stiffness. For this reason, it is important to apply conditioning load cycles prior to testing to determine the in situ resilient modulus. Once surface paving is complete, the pavement foundation below is confined by the overlying pavement layers. The response of a pavement foundation to subsequent repeated traffic loading is both nonlinear and stress-dependent, and therefore the effect of confinement is an important condition to consider in a field-based M_r test.

    - FWD testing provides an estimate of the modulus of the asphalt layer, but this value is not the same as the stress- and frequency-dependent dynamic modulus value used in the design of the asphalt layer.

- The results demonstrated the importance of support conditions on the overall composite response at the surface under loading. Improved support at the subgrade level with cement stabilization provided the best response to loading at the surface, followed by cement

stabilization at the granular base layer level. Although the geosynthetic-stabilized test sections did not show modulus values as high as the cement-stabilized test sections, experience has shown that sections with geosynthetic reinforcement exhibit better resistance against permanent deformation/rutting under traffic loading than sections without reinforcement. This aspect was not evaluated at this site and must be evaluated in future testing.

- Although sections with cement stabilization exhibited improved support conditions compared to sections without stabilization, the stabilization did not improve uniformity. Specifically, the coefficient of variation (COV) of modulus values in the cement-stabilized sections was higher than in the sections without cement stabilization, and this is related to a lack of construction process control for this stabilization process.

Based on the lessons learned and the limitations identified above, White et al. (2018) recommended the following for consideration by the Iowa DOT for future testing and evaluation at this site:

- Evaluate new in situ testing technologies that provide a direct measurement of the M_r values and *k*-values of the foundation layers and the stress- and frequency-dependent dynamic modulus values of the asphalt layers. The objective of such testing and evaluation should be to generate typical foundation input parameter values that can be used in future design by the Iowa DOT.

- Evaluate the test sections over the long term (10+ years) and/or with accelerated pavement testing (trafficking or accelerated loading) to evaluate the influence of the foundation layers on the permanent deformation behavior at the surface.

- Evaluate the condition of the temperature monitoring sensors and continue the monitoring to generate frost-depth penetration data over a longer period.

In Situ Direct Measurement of Modulus Using Automated Plate Load Testing

In situ foundation support values (i.e., resilient modulus [M_r], modulus of subgrade reaction [k-value], and permanent deformation [δ_p]) have not been traditionally directly measured. The mechanistic-empirical calibration process for foundation input parameters is primarily empirical and relies upon limited and often time-consuming laboratory testing and the adoption of conservative values (AASHTO 2010, Darter et al. 2014, Mallela et al. 2013). Even with modern laboratory testing of foundation materials, various challenges limit the understanding of in situ conditions, as highlighted in Figure 14. In situ plate load testing overcomes many of these limitations.

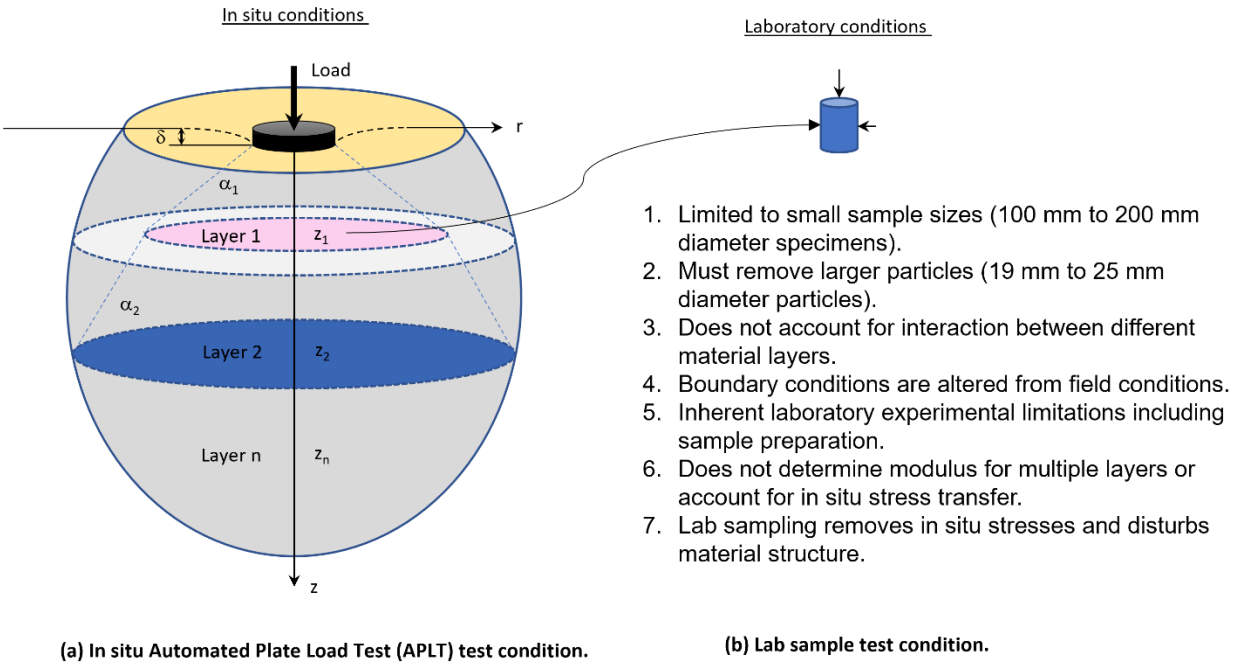

White et al. 2019a

Figure 14. APLT in comparison to limitations of laboratory testing

Plate load testing is considered the long standing "gold standard" for assessing in situ pavement foundation support conditions. From the 1930s to 1980s, the Bureau of Public Roads, the U.S. Army Corps of Engineers, American Association of State Highway Officials (AASHO), and several state agencies used plate load testing (Teller and Sutherland 1935, U.S. Army Corps of Engineers 1943, AASHO 1962) to determine k-values for airfield and highway applications, investigate concrete pavement behavior, and verify/calibrate design equations. In the 1940s, the Bureau of Public Roads reported extensive field testing from the Arlington Experiment Farm in Virginia, which involved plate load tests with repeated load-unload cycles (Teller and Sutherland 1943). The AASHO Road Test also included repeated load-unload plate load testing to determine k-values for rigid pavements and resilient modulus M_r (using a k-M_r theoretical relationship) for flexible pavements.

The pioneering efforts from the 1930s to the 1980s established plate load testing to determine the load-displacement relationship of foundation layers and played a significant role in calibrating the pavement thickness design equations developed by the American Association of State Highway and Transportation Officials (AASHTO), Portland Cement Association (PCA), and U.S. Army Corps of Engineers. However, the *manual* methods were time consuming because of significant setup times with heavy reaction loads, often creating unsafe conditions. Also, without automation, obtaining reproducible results from manual testing can be difficult because of operator bias, lack of control over maintaining and applying loads, etc., even for a static test. It is almost impractical to apply repeated loads with a controlled load pulse using manual methods.

Because of those limitations, the frequency with which plate load tests were conducted has diminished substantially. As a simplification, several agencies attempted to develop local

empirical relationships between plate load test measurements and CBR values, R-values, FWD results, and other measurements. These empirical relationships, however, present significant uncertainties and often poorly match the field conditions.

In response to the very important role of plate load testing for pavement foundation characterization, the limitations involved with manual setup, and the uncertainties associated with using empirical relationships, the modern APLT system was developed (Figure 15). With APLT, it is now possible to obtain direct and rapid measurement of pavement foundation support values. APLT technology, although relatively new, has been used in recent years on several pavement projects (see White and Vennapusa 2017, Vennapusa et al. 2018, White et al. 2019a, White et al. 2019b) and was selected for deployment in Iowa to assist with the determination of foundation support values as part of the Iowa DOT's ongoing statewide calibration efforts.

White et al. 2019a

Figure 15. APLT setup at a project site on US 20 in Sac County, Iowa, in October 2017

To obtain the AASHTOWare Pavement ME Design input data needed for typical Iowa foundation layers, the Iowa DOT selected the APLT to conduct a statewide field study as part of the State Transportation Innovation Councils (STIC) initiative. A total of 10 project sites were selected that covered common unbound foundation layer cross sections used in Iowa highways. Projects consisted of different subbase types (granular subbase and modified subbase), different subbase materials (crushed limestone and recycled concrete aggregate), and different subgrade types (select subgrade and embankment cut/fill subgrade).

The goal at each site was to perform cyclic APLTs at four to eight test locations using a 12 in. diameter loading plate (Figure 16) and perform static APLTs using a 30 in. diameter loading plate (Figure 17) to determine modulus of subgrade reaction *k*-values at one to two test locations. Results and findings from the study are summarized in White et al. (2019a).

White et al. 2019a

Figure 16. 12 in. diameter loading plate setup for cyclic APLT to measure composite and layered resilient modulus values

White et al. 2019a

Figure 17. 30 in. diameter loading plate setup for static APLT to measure modulus of subgrade reaction values

Key findings from the STIC project are as follows:

- Typical values provided in AASHTOWare Pavement ME Design based on soil classification can significantly underestimate or overestimate the M_r values. Therefore, it is important to perform field measurements for verification of design input parameters.

- The cyclic APLTs showed that the M_r values on the unbound layers are variable across the state and within a given project site. The COV at each site ranged from 7% to 70%. For

reference, a COV of about 20% is typically considered a relatively uniform condition. Results from 6 out of the 10 projects yielded a COV greater than 20%.

- The use of 2 ft of special backfill to improve the subgrade at one of the project sites provided higher M_r values than measured at other projects, and the special backfill material layer (consisting of RAP) increased in stiffness between test periods.

- The modulus of subgrade reaction *k*-values obtained across the state varied between 35 pci to 300 pci. Of the 14 tests performed across the state, 11 showed *k* values lower than 150 pci, which is the typically assumed (conservative) design input target value by the Iowa DOT for PCA (1984) design. At one site, two tests performed on the compacted modified subbase layer about 420 ft apart showed drastically different *k*-values of 39 and 284 pci.

- The *k*-values obtained over granular subbase/modified subbase layers were on average lower than the *k*-values obtained directly on the underlying subgrade layer. This finding suggests that the subbase layers were relatively loose/uncompacted at the surface, which is also evidenced by the relatively high reload to initial load *k*-value ratio (k_2/k_1). Six out of seven tests on subbase layers produced ratios greater than 3. For reference, Swedish specifications require the ratio of reload to initial moduli values to be less than 2.8 for base/subbase layers within the top 0 to 10 in. as an indicator of compaction quality.

- Permanent or plastic deformations occurring from repeated traffic loading is a recognized cause of pavement distresses. To quantify this factor, the permanent deformation δ_p was monitored and reported for the cyclic and static APLTs. The average δ_p at each site varied between 0.01 and 0.26 in., and the COV at each site varied between 14% and 123%. The δ_p values at the end of the static APLTs varied between 0.05 and 0.4 in. Out of the 14 static APLTs, 11 showed δ_p values greater than 0.05 in., which is considered the critical limit to develop loss of support beneath pavement. A plot of *k*-values versus δ_p values from the STIC project and several recent projects (between 2019 to 2022) across Iowa for the various materials involved is provided in Figure 18.

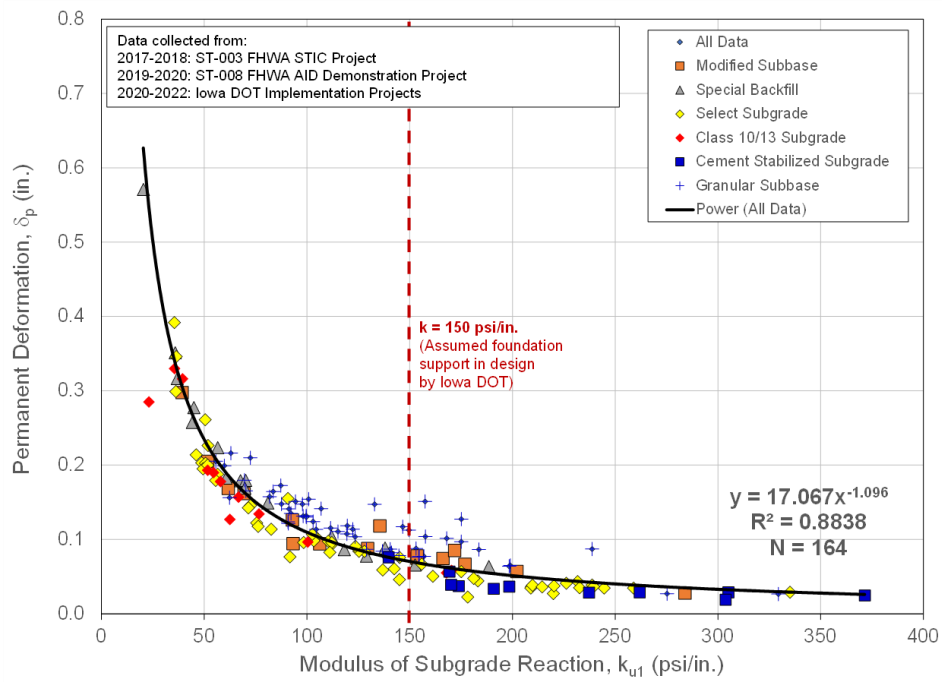

Gieselman et al. 2023

Figure 18. Modulus of subgrade reaction (*k*-value) versus permanent deformation at the end of testing from field static plate load test measurements (164 tests from multiple project sites across Iowa from 2017 to 2022)

APLTs can be performed directly on the foundation layers, on the pavement layers, and through a core hole under the existing pavement layers. Figure 19 shows a cyclic APLT being conducted using a 12 in. diameter loading plate on a foundation layer beneath existing pavement using a 14 in. diameter core hole. Similarly, Figure 20 shows testing using a 30 in. diameter loading plate setup on a foundation layer beneath existing pavement.

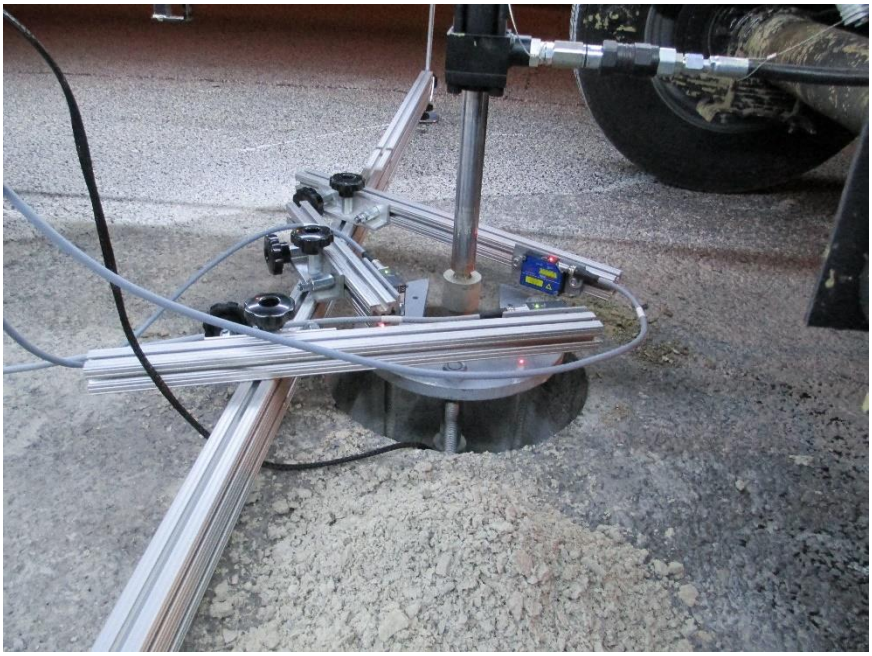

Figure 19. 12 in. diameter loading plate setup for cyclic APLT to measure resilient modulus values under an existing pavement in a core hole

Figure 20. 30 in. diameter loading plate setup for static APLT to measure modulus of subgrade reaction values under an existing pavement in a core hole

PROPOSED EXPERIMENTAL PLAN

The Phase IV performance evaluation testing program presented herein was developed after a review of the Phase I through III field and laboratory test results and analysis documented in White et al. (2018). The variability observed within each test section, between the test sections, and between tests performed in each season for the measured in situ FWD modulus values was considered in selecting the minimum number of tests for each section. The testing program was developed with the goal of *direct* measurement of the in situ mechanistic input parameters that are necessary in AASHTOWare Pavement ME Design, along with the impacts of seasonal variations in the measurement values.

In the sections below, justifications are provided for the number of tests required for each section, the test sections selected for Phase IV evaluation, and the proposed test measurements with an explanation of the engineering measurement values that will be obtained.

Determination of Minimum Number of Tests

Statistical determination of the minimum number of measurements requires knowledge of the COV within a sample group and the difference between the mean values of the selected sample groups. Belle (2008) provides a "rule of thumb" calculation based on the COV and the expected percentage change in mean values (μ_o and μ_1) within each sample group (equation [1]). A sample size matrix showing the number of tests required using equation (1) is provided in Table 3.

$$n = \frac{16\,COV^2}{(ln\mu_0 - ln\mu_1)^2} \quad (1)$$

Table 3. Sample size matrix (number of tests required) for a range of COVs and percentage changes in means between two sample groups

Ratio of Means		0.95	0.90	0.85	0.80	0.70	0.60	0.50
% Change		5	10	15	20	30	40	50
Coefficient of Variation (%)	5	16	4	2	1	1	1	1
	10	61	15	7	4	2	1	1
	15	137	33	14	8	3	2	1
	20	244	58	25	14	6	3	2
	30	548	130	55	29	12	6	3
	40	974	231	97	52	21	10	6
	50	>1000	361	152	81	32	16	9
	75	>1000	811	341	181	71	35	9
	100	>1000	>1000	606	322	126	62	34

Source: Modified from Belle 2008

The number of test values highlighted in Table 3 is the range of values selected as applicable for Phase IV testing considering the observed variability in the Phase I through III test results, engineering judgement, and the time and cost involved in obtaining the different measurements.

Selected Test Sections

Summaries of the test section information along the 12 roads oriented in the north-south direction (denoted as 1st St. to 12th St.) and the 3 roads in the east-west direction (denoted as South Ave., Central Ave., and North Ave.), along with the numbers of tests for the minimum and comprehensive scopes of proposed work, are presented in Tables 4 and 5, respectively. The minimum proposed scope of work includes fewer tests compared to the comprehensive scope. The minimum proposed scope is the minimum amount of work recommended considering the total cost of the testing program. The following foundation layer stabilization methods are included in the evaluation:

- Woven and nonwoven geotextile at subgrade/subbase interface
- Triaxial and biaxial geogrid at subgrade/subbase interface
- PC stabilization of subgrade (10% PC)
- FA stabilization of subgrade (10% and 20% FA)
- PC stabilization of reclaimed subbase (reclaimed from existing granular subbase layer on site)
- PC + fiber stabilization of recycled subbase with white PP fibers
- PC + fiber stabilization of reclaimed subbase with black MF-PP fibers
- Mechanical stabilization (mixing subgrade with reclaimed subbase)
- Reclaimed subbase between MSB and subgrade
- High-energy impact compaction of subgrade

In addition, some test sections (i.e., 6th St. South and 11th St. North) included a geocomposite drainage layer (GCDL) at the pavement/subbase interface, with a portion of those sections built without the GCDL for comparison. Permeability tests are selected in those areas for comparison.

APLT and core hole permeability (CHP) tests were selected as field testing methods to be used in this Phase IV evaluation. At each of the test locations, a DCP test will also be performed. An illustration of the proposed tests and the measurement influence depths is provided in Figure 21. These tests will be initiated in fall 2023 followed by testing in spring 2024, fall 2024, and spring 2025.

APLT Test A is a cyclic test performed on the pavement layer. APLT Tests B and C are performed directly on the pavement foundation layer through a 14 in. diameter core hole in the pavement layer. The CHP test is performed in a 6 in. diameter core hole in the pavement. The cores will be drilled and extracted by the research team. The test methods are described in more detail in the following section of the report. After testing, the pavement cores will be replaced in the core holes and sealed so they can be accessed again for follow-up testing.

Table 4. Summary of test sections, with highlighted sections selected for Phase IV testing, and proposed number of tests to be repeated in each season – minimum recommended test plan

Street	Section	Station	Pavement	Subbase Layer[b]	Subgrade Improvement and Profile[a]	Proposed No. of Tests			
						APLT			
						Test A	Test B	Test C	CHP
1st	South	100+12.00 to 106+86.00	2 in. HMA + 4 in. HMA	6 in. (5.5 in. actual) MSB	12 in. compacted subgrade	0	0	0	0
	North	107+14.00 to 113+88.00	2 in. HMA + 4 in. HMA			0	0	0	0
2nd	South	200+12.00 to 206+86.00	2 in. HMA + 4 in. HMA	6 in. (6.1 in. actual) MSB	12 in. mechanically stabilized subgrade	2	1	1	0
	North	207+14.00 to 213+88.00	2 in. HMA + 4 in. HMA			2	1	1	0
3rd	South	300+12.00 to 306+86.00	2 in. WMA + 4 in. WMA	1 in. MSB	6 in. geocell reinforced MSB, NW geotextile	0	0	0	0
	North	307+14.00 to 313+88.00	2 in. HMA + 4 in. HMA	2 in. MSB	4 in. geocell reinforced MSB, NW geotextile	0	0	0	0
4th	South	400+12.00 to 406+86.00	2 in. WMA + 4 in. WMA	6 in. (7.0 in. actual) MSB	Woven geotextile	2	1	1	0
	North	407+14.00 to 413+88.00	2 in. WMA + 4 in. WMA	6 in. (7.0 in. actual) MSB	NW geotextile	2	1	1	0
5th	South	500+12.00 to 506+86.00	2 in. WMA + 4 in. WMA	6 in. (5.8 in. actual) MSB	Biaxial geogrid	2	1	1	0
	North	507+14.00 to 513+88.00	2 in. WMA + 4 in. WMA	6 in. (5.8 in. actual) MSB	Triaxial geogrid	2	1	1	0
6th	South	4020+82.30 to 4026+65.49	6 in. PCC + GCDL	6 in. (4.5 to 5 in. actual) MSB	6 in. reclaimed subbase + 5% (5.5% actual) PC + 0.4% (0.5% actual) MF-PP fibers	2	1	1	0
		4020+21.30 to 4020+82.30	6 in. PCC + GCDL		6 in. reclaimed subbase + 0.4% (0.4% actual) MF-PP fibers	1	1	1	1
	North	4026+93.49 to 4032.85.49	6 in. PCC	6 in. (4.5 to 5 in. actual) MSB	6 in. reclaimed subbase + 5% (5.6% actual) PC + 0.4% (0.5% actual) PP fibers	2	1	1	1
		4032+85.49 to 4033+67.49	6 in. PCC		6 in. reclaimed subbase + 0.4% (0.5% actual) PP fibers	1	1	1	0

Street	Section	Station	Pavement	Subbase Layer[b]	Subgrade Improvement and Profile[a]	Proposed No. of Tests			
						APLT			
						Test A	Test B	Test C	CHP
7th	South	700+12.00 to 706+86.00	2 in. HMA + 4 in. HMA	6 in. (5.5 in. actual) MSB	6 in. reclaimed subbase + 5% (5.2% actual) PC	2	0	0	0
	North	707+14.00 to 713+88.00	2 in. HMA + 4 in. HMA	6 in. (5.5 in. actual) MSB	6 in. reclaimed subbase + 5% (6.2% actual) PC	2	1	1	0
8th	South	800+12.00 to 806+86.00	2 in. HMA + 4 in. HMA	6 in. (6.0 in. actual) MSB	Compacted subgrade[d]	2	1	1	1
	North	807+14.00 to 813+88.00	2 in. HMA + 4 in. HMA	6 in. (6.0 in. actual) MSB	Compacted subgrade	2	1	1	1
9th	South	900+12.00 to 906+86.00	2 in. WMA + 4 in. WMA	6 in. (6.0 in. actual) MSB	6 in. reclaimed subbase	2	0	0	0
	North	907+14.00 to 913+88.00	2 in. HMA + 4 in. HMA	6 in. (6.0 in. actual) MSB	6 in. reclaimed subbase	2	1	1	0
10th	South	1000+12.00 to 1006+86.00	2 in. WMA + 4 in. WMA	6 in. (5.5 in. actual) MSB	Existing subgrade (Control)	2	1	1	0
	North	1007+14.00 to 1013+88.00	2 in. WMA + 4 in. WMA	6 in. (5.5 in. actual) MSB	12 in. compacted subgrade[c]	2	1	1	0
11th	South	1100+12.00 to 1106+86.00	2 in. WMA + 4 in. WMA	6 in. (6.0 in. actual) MSB	12 in. 20% (22.3% actual) Port Neal FA stabilized subgrade	2	1	1	0
	North	1107+14.00 to 1108+00 (approx.)	2 in. WMA + 4 in. WMA	6 in. (6.0 in. actual) MSB	12 in. 10% (11.4% actual) PC stabilized subgrade	2	0	0	1
		1108+00 to 1113+88.00	2 in. WMA + 4 in. WMA + GCDL			2	1	1	1
12th	South	1200+12.00 to 1204+46.00	2 in. HMA + 4 in. HMA	6 in. (6.0 in. actual) MSB	12 in. 10% (10% actual) Port Neal FA stabilized subgrade	2	1	1	0
		1204+46.00 to 1206+86.00			12 in. 10% (10% actual) Muscatine FA stabilized subgrade	2	1	1	0
	North	1207+14.00 to 1213+88.00	2 in. HMA + 4 in. HMA	6 in. (5.7 in. actual) MSB	12 in. 15% (15.8% actual) Ames FA stabilized subgrade	2	1	1	0

Street	Section	Station	Pavement	Subbase Layer[b]	Subgrade Improvement and Profile[a]	Proposed No. of Tests			
						APLT			
						Test A	Test B	Test C	CHP
North Ave	West[e]	3000+02.50 to 3002+02.50	6 in. PCC	9 in. MSB	6 in. reclaimed subbase, biaxial geogrid	0	0	0	0
	West[e]	3002+02.50 to 3004+02.50	6 in. PCC	9 in. MSB	6 in. reclaimed subbase, triaxial geogrid	0	0	0	0
	East[e]	3004+02.50 to 3023+38.14	6 in. PCC	9 in. MSB	6 in. reclaimed subbase	0	0	0	0
South Ave.	West[e]	1001+00.00 to 1003+00.00	6 in. PCC	9 in. MSB[f]	6 in. reclaimed subbase, biaxial geogrid	0	0	0	0
		1003+00.00 to 1005+00.00	6 in. PCC		6 in. reclaimed subbase, biaxial geogrid	0	0	0	0
		1005+00.00 to 1009+06.08	6 in. PCC		6 in. reclaimed subbase	0	0	0	0
South Ave.	East[e]	1009+94.00 to 1011+94.00	6 in. PCC	9 in. MSB[f]	6 in. reclaimed subbase, biaxial geogrid	0	0	0	0
		1011+94.00 to 1013+94.00	6 in. PCC		6 in. reclaimed subbase, biaxial geogrid	0	0	0	0
		1013+94.00 to 1023+39.91	6 in. PCC		6 in. reclaimed subbase	0	0	0	0
Central Ave.	East/ West[e]	2000+01.43 to 2023+39.59	6 in. PCC	9 in. MSB[f]	6 in. reclaimed subbase	0	0	0	0
TOTAL Number of Tests						**46**	**21**	**21**	**6**

Notes:
[a] Thicknesses provided are nominal unless indicated as actual in parenthesis (actual measurements were obtained from shallow excavations).
[b] MSB layer composed of crushed limestone unless otherwise noted.
[c] Existing subgrade scarified, moisture conditioned, and compacted.
[d] The original subbase layer topped with chip seal was compacted with a high-energy impact roller, and the subbase layer was excavated down to about 6 in. below final grade and replaced with MSB.
[e] With reference to 6th St.
[f] Mixture of recycled PCC and asphalt

Table 5. Summary of test sections, with highlighted sections selected for Phase IV testing, and proposed number of tests to be repeated each season – comprehensive test plan

Street	Section	Station	Pavement	Subbase Layer[b]	Subgrade Improvement and Profile[a]	Proposed No. of Tests			
						APLT			
						Test A	Test B	Test C	CHP
1st	South	100+12.00 to 106+86.00	2 in. HMA + 4 in. HMA	6 in. (5.5 in. actual) MSB	12 in. compacted subgrade	0	0	0	0
	North	107+14.00 to 113+88.00	2 in. HMA + 4 in. HMA			0	0	0	0
2nd	South	200+12.00 to 206+86.00	2 in. HMA + 4 in. HMA	6 in. (6.1 in. actual) MSB	12 in. mechanically stabilized subgrade	3	1	1	0
	North	207+14.00 to 213+88.00	2 in. HMA + 4 in. HMA			3	1	1	0
3rd	South	300+12.00 to 306+86.00	2 in. WMA + 4 in. WMA	1 in. MSB	6 in. geocell reinforced MSB, NW geotextile	0	0	0	0
	North	307+14.00 to 313+88.00	2 in. HMA + 4 in. HMA	2 in. MSB	4 in. geocell reinforced MSB, NW geotextile	0	0	0	0
4th	South	400+12.00 to 406+86.00	2 in. WMA + 4 in. WMA	6 in. (7.0 in. actual) MSB	Woven geotextile	6	1	1	0
	North	407+14.00 to 413+88.00	2 in. WMA + 4 in. WMA	6 in. (7.0 in. actual) MSB	NW geotextile	6	1	1	0
5th	South	500+12.00 to 506+86.00	2 in. WMA + 4 in. WMA	6 in. (5.8 in. actual) MSB	Biaxial geogrid	6	1	1	0
	North	507+14.00 to 513+88.00	2 in. WMA + 4 in. WMA	6 in. (5.8 in. actual) MSB	Triaxial geogrid	6	1	1	0
6th	South	4020+82.30 to 4026+65.49	6 in. PCC + GCDL	6 in. (4.5 to 5 in. actual) MSB	6 in. reclaimed subbase + 5% (5.5% actual) PC + 0.4% (0.5% actual) MF-PP fibers	4	1	1	0
		4020+21.30 to 4020+82.30	6 in. PCC + GCDL		6 in. reclaimed subbase + 0.4% (0.4% actual) MF-PP fibers	2	1	1	1
	North	4026+93.49 to 4032.85.49	6 in. PCC	6 in. (4.5 to 5 in. actual) MSB	6 in. reclaimed subbase + 5% (5.6% actual) PC + 0.4% (0.5% actual) PP fibers	4	1	1	1
		4032+85.49 to 4033+67.49	6 in. PCC		6 in. reclaimed subbase + 0.4% (0.5% actual) PP fibers	2	1	1	0

Street	Section	Station	Pavement	Subbase Layer[b]	Subgrade Improvement and Profile[a]	Proposed No. of Tests			
						APLT			
						Test A	Test B	Test C	CHP
7th	South	700+12.00 to 706+86.00	2 in. HMA + 4 in. HMA	6 in. (5.5 in. actual) MSB	6 in. reclaimed subbase + 5% (5.2% actual) PC	3	0	0	0
	North	707+14.00 to 713+88.00	2 in. HMA + 4 in. HMA	6 in. (5.5 in. actual) MSB	6 in. reclaimed subbase + 5% (6.2% actual) PC	3	1	1	0
8th	South	800+12.00 to 806+86.00	2 in. HMA + 4 in. HMA	6 in. (6.0 in. actual) MSB	Compacted subgrade[d]	2	1	1	1
	North	807+14.00 to 813+88.00	2 in. HMA + 4 in. HMA	6 in. (6.0 in. actual) MSB	Compacted subgrade	2	1	1	1
9th	South	900+12.00 to 906+86.00	2 in. WMA + 4 in. WMA	6 in. (6.0 in. actual) MSB	6 in. reclaimed subbase	3	0	0	0
	North	907+14.00 to 913+88.00	2 in. HMA + 4 in. HMA	6 in. (6.0 in. actual) MSB	6 in. reclaimed subbase	3	1	1	0
10th	South	1000+12.00 to 1006+86.00	2 in. WMA + 4 in. WMA	6 in. (5.5 in. actual) MSB	Existing subgrade (Control)	6	1	1	0
	North	1007+14.00 to 1013+88.00	2 in. WMA + 4 in. WMA	6 in. (5.5 in. actual) MSB	12 in. compacted subgrade[c]	6	1	1	0
11th	South	1100+12.00 to 1106+86.00	2 in. WMA + 4 in. WMA	6 in. (6.0 in. actual) MSB	12 in. 20% (22.3% actual) Port Neal FA stabilized subgrade	6	1	1	0
	North	1107+14.00 to 1108+00 (approx.)	2 in. WMA + 4 in. WMA	6 in. (6.0 in. actual) MSB	12 in. 10% (11.4% actual) PC stabilized subgrade	2	0	0	1
		1108+00 to 1113+88.00	2 in. WMA + 4 in. WMA + GCDL			4	1	1	1
12th	South	1200+12.00 to 1204+46.00	2 in. HMA + 4 in. HMA	6 in. (6.0 in. actual) MSB	12 in. 10% (10% actual) Port Neal FA stabilized subgrade	3	1	1	0
		1204+46.00 to 1206+86.00			12 in. 10% (10% actual) Muscatine FA stabilized subgrade	3	1	1	0
	North	1207+14.00 to 1213+88.00	2 in. HMA + 4 in. HMA	6 in. (5.7 in. actual) MSB	12 in. 15% (15.8% actual) Ames FA stabilized subgrade	6	1	1	0

Street	Section	Station	Pavement	Subbase Layer[b]	Subgrade Improvement and Profile[a]	Proposed No. of Tests			
						APLT			
						Test A	Test B	Test C	CHP
North Ave	West[e]	3000+02.50 to 3002+02.50	6 in. PCC	9 in. MSB	6 in. reclaimed subbase, biaxial geogrid	0	0	0	0
	West[e]	3002+02.50 to 3004+02.50	6 in. PCC	9 in. MSB	6 in. reclaimed subbase, triaxial geogrid	0	0	0	0
	East[e]	3004+02.50 to 3023+38.14	6 in. PCC	9 in. MSB	6 in. reclaimed subbase	0	0	0	0
South Ave.	West[e]	1001+00.00 to 1003+00.00	6 in. PCC	9 in. MSB[f]	6 in. reclaimed subbase, biaxial geogrid	0	0	0	0
		1003+00.00 to 1005+00.00	6 in. PCC		6 in. reclaimed subbase, biaxial geogrid	0	0	0	0
		1005+00.00 to 1009+06.08	6 in. PCC		6 in. reclaimed subbase	0	0	0	0
South Ave.	East[e]	1009+94.00 to 1011+94.00	6 in. PCC	9 in. MSB[f]	6 in. reclaimed subbase, biaxial geogrid	0	0	0	0
		1011+94.00 to 1013+94.00	6 in. PCC		6 in. reclaimed subbase, biaxial geogrid	0	0	0	0
		1013+94.00 to 1023+39.91	6 in. PCC		6 in. reclaimed subbase	0	0	0	0
Central Ave.	East/ West[e]	2000+01.43 to 2023+39.59	6 in. PCC	9 in. MSB[f]	6 in. reclaimed subbase	0	0	0	0
TOTAL Number of Tests						**94**	**21**	**21**	**6**

Notes:
[a] Thicknesses provided are nominal unless indicated as actual in parenthesis (actual measurements were obtained from shallow excavations).
[b] MSB layer composed of crushed limestone unless otherwise noted.
[c] Existing subgrade scarified, moisture conditioned, and compacted.
[d] The original subbase layer topped with chip seal was compacted with a high-energy impact roller, and the subbase layer was excavated down to about 6 in. below final grade and replaced with MSB.
[e] With reference to 6th St.
[f] Mixture of recycled PCC and asphalt

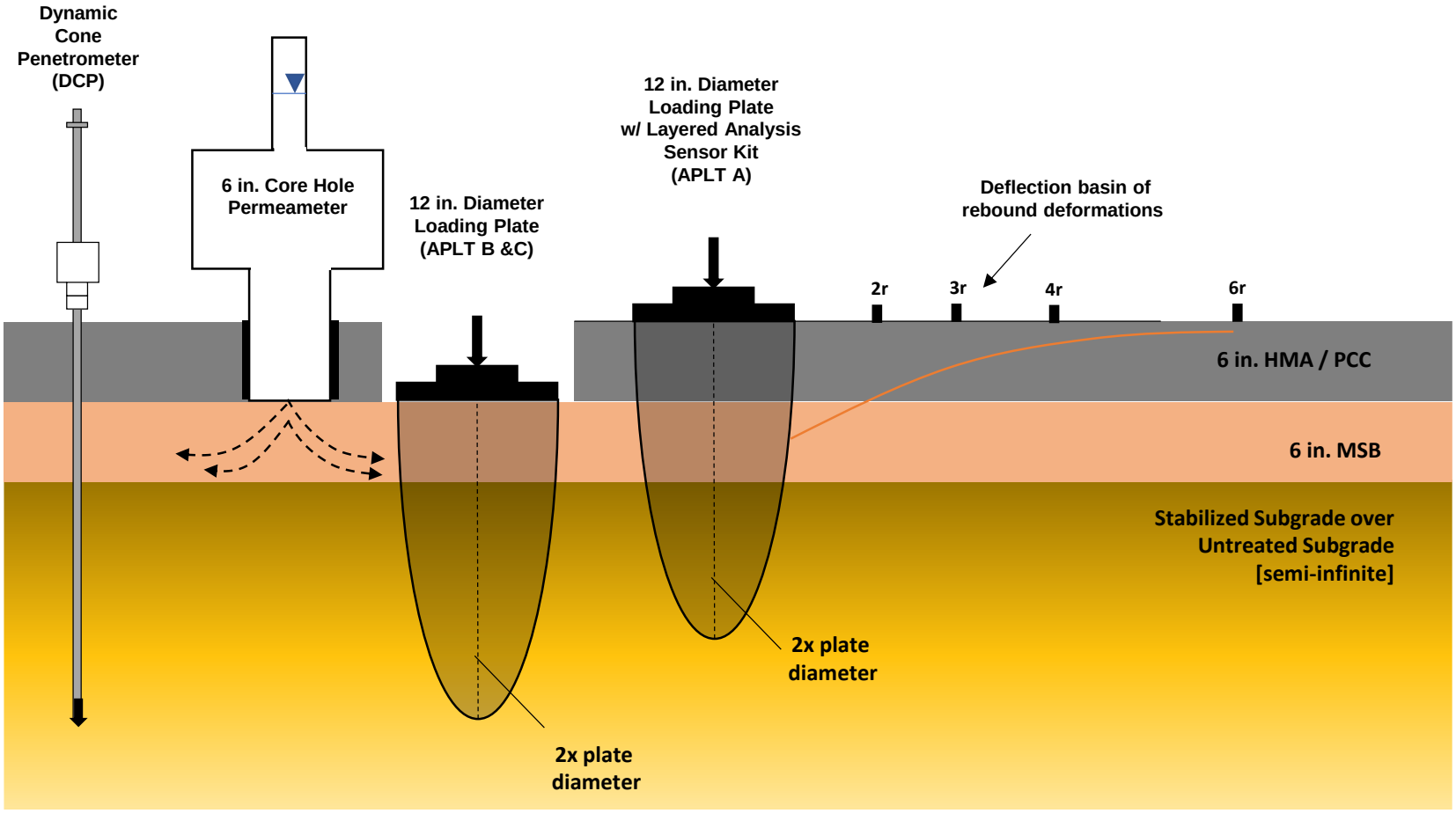

Figure 21. Different tests and their measurement influence depths

Proposed Field Testing

Automated Plate Load Testing

Three APLT methods (A, B, and C) are proposed, and the engineering measurement values that will be obtained using each method are described below.

Test A – EXTCY-PS-High-12_Layered

This is a nondestructive cyclic plate load test performed on an HMA or PCC pavement surface (Figure 22) and involves applying controlled cyclic stress by maintaining a constant contact stress between the plate and the test surface.

Figure 22. 12 in. diameter loading plate setup with layered analysis sensor kit on asphalt pavement surface

The load-deformation response of the loading plate and the deformation bowl away from the plate is measured. The following test parameters are proposed:

- 12 in. diameter loading plate
- 80 psi cyclic stress representing AASHTO W18 (18-kip) axle loading over a single tire with an equivalent area of 12 in. diameter, for 150 loading cycles, using 0.2 sec loading time and 0.8 sec dwell time

- Rebound deformations measured at r, 2r, 3r, 4r, and 6r (r = plate radius)
- Permanent deformation measured at r

The engineering measurement values to be reported from the test include the following:

- Composite resilient modulus ($M_{r\text{-}comp}$), which provides a measure of the composite response of the pavement layer and the supporting layers under dynamic loading, using the modified Boussinesq's elastic half-space solution with applied cyclic stress and plate rebound deformations
- Layered modulus values using APLT-BACK (White et al. 2019b) for the pavement layer and the underlying foundation layers (modified subbase and subgrade layers). APLT-BACK is an advanced proprietary software program developed in March 2017 by Ingios Geotechnics, Inc. A shortcoming of other currently available back-calculation software programs is that they model the loading by assuming a flexible plate with a uniform stress distribution. However, the assumption of a uniform stress distribution is not accurate because of the rigidity of the plate. The APLT-BACK program addresses this issue by modeling the loading on a rigid (or semi-rigid) plate with constant deformation beneath the plate. This feature is considered a significant advancement over other software used as part of the current state of the practice (e.g., FAA 2009).
- Permanent deformation forecasting regression model based on number of loading cycles

The temperature of the asphalt surface layer influences the plate deformation because of the temperature-dependent nature of the asphalt mixtures (AASHTO 1986). Empirical correction factors are provided in AASHTO (1986) standardized to a temperature of 68°F and are dependent on the asphalt layer thickness. Mid-layer ("mat") temperatures are needed to apply these correction factors. Mid-layer temperatures will be measured using the on-site temperature instrumentation on 5th St. if they can be located (the datalogger was removed and the area paved over); otherwise, new sensors may be installed. In addition, the results will be compared with the traditionally used BELLS2 prediction model (per Lukanen et al. 2000) using the surface temperature measurements and the previous day's average one-day temperature for comparison purposes.

Test B – INCST-PF-Low-12_Layered

This is a static plate load test performed directly on the underlying foundation layer through a core hole made in the pavement layer (see Figure 19). A 14 in. diameter core hole will be required to perform this test. The test is performed using a plate and reference beam setup per ASTM D1195 and ASTM D1196 using two loading cycles. The following test parameters are proposed:

- 12 in. diameter loading plate
- Seating stress of 1 psi
- Incremental loading up to a maximum of 25 psi in 5 psi increments (0, 5, 10, 15, 20, and 25)
- Two load/unload cycles to determine initial and reload modulus

- Maintenance of each load increment for at least 3 minutes after a deformation rate of 0.001 in./minute is achieved (per ASTM D1195 and ASTM D1196), or a maximum of 10 minutes during the initial load cycle and a maximum of 5 minutes during the reload cycle, whichever occurs first

The engineering measurement values to be reported from the test include the following:

- Modulus of subgrade reaction (*k*-value) for the initial and reload cycles for a 12 in. diameter loading plate and for a 30 in. diameter loading plate using plate size corrections (per Terzaghi 1955)
- Ratio of reload to initial load *k*-value

Test C – RDCY-PF-Low-12_1000_Composite

This cyclic plate load test will be performed immediately after Test B in the same core hole. The advantage of this test is that it provides measurements for validation of the layered analysis results obtained using Test A and "universal" model parameter results that are applicable in Level 1 AASHTOWare Pavement ME Design for foundation layers.

The following test parameters are proposed:

- 12 in. diameter loading plate
- 1,000 loading cycles using Ingios' random loading sequence (RDL) using 10 different cyclic stress levels (5 to 50 psi cyclic stresses at 5 psi increments), with a 2 psi contact stress (see Table 5)
- Plate deformations (rebound and permanent) measured at r

Table 5. RDL load sequence testing plan

Test Designation	Percent Distribution	Number of cycles, N [per 100 cycle set]	Cyclic Stress, σ_{cyclic} [psi]	Minimum Stress, σ_{min} [psi]	Maximum Stress, σ_{max}	Plate Configuration/Notes
C [1,000 cycles]	5%	5	5	2	7	12 in. diameter flat plate with deflection readings of the plate. 0.2 second load time and 0.8 second dwell time.
	8%	8	10	2	12	
	15%	15	15	2	17	
	22%	22	20	2	22	
	16%	16	25	2	27	
	12%	12	30	2	32	
	9%	9	35	2	37	
	6%	6	40	2	42	
	5%	5	45	2	47	
	2%	2	50	2	52	

The engineering measurement values to be reported from the test include the following:

- Stress-dependent composite resilient modulus ($M_{r\text{-}comp}$) for each loading cycle (see example results in Figure 23) using the modified Boussinesq's elastic half-space solution with applied cyclic stress and plate rebound deformations
- "Universal" model parameters for predicting M_r values along with permanent deformation model parameters (see Figure 24)

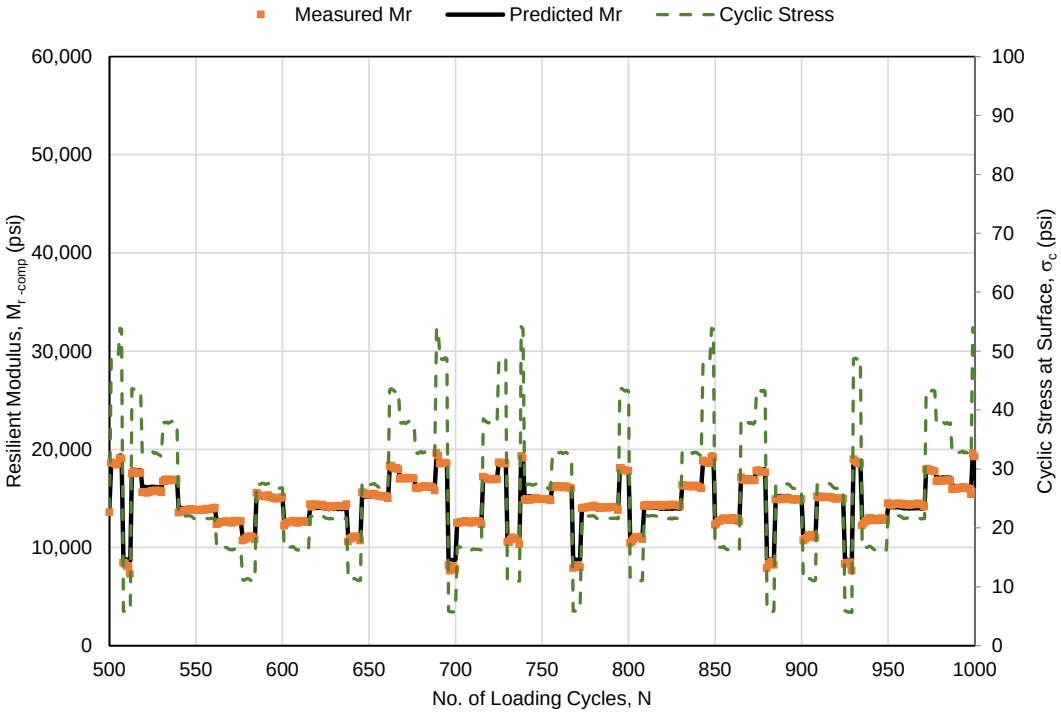

Figure 23. Example dataset using RDL results showing applied cyclic stress and measured versus predicted M_r values over 500 loading cycles

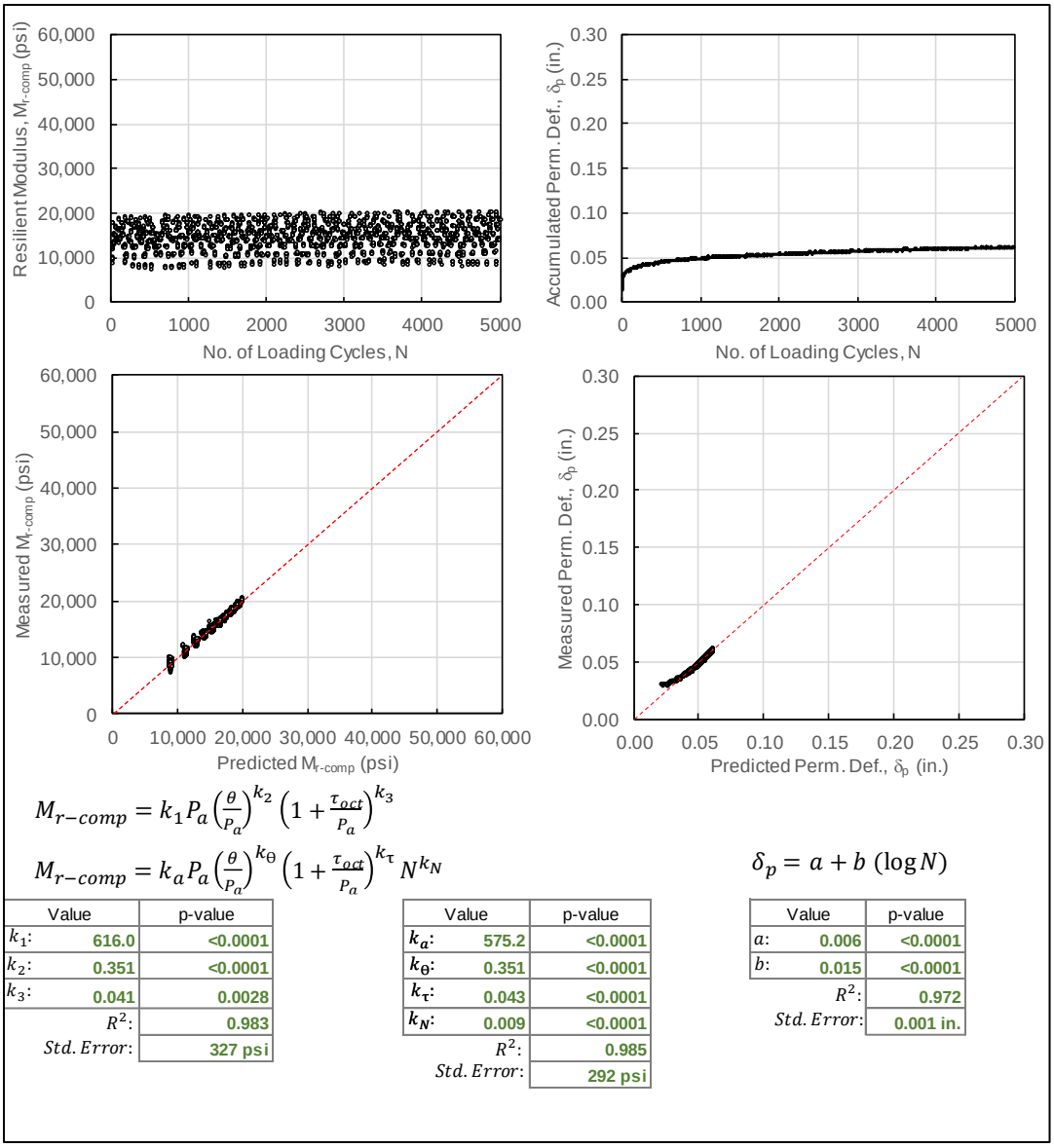

Figure 24. Example regression model results for predicting $M_{r\text{-}comp}$ and permanent deformation from RDL test

Core Hole Permeability Test

The CHP test device was developed at Iowa State University (ISU) and was implemented recently for Iowa DOT research projects (White and Vennapusa 2014). The test procedure involves coring a 6 in. diameter hole in the pavement down to the underlying support layer. The CHP device is inserted into the core hole and sealed at the bottom of the device and against the interior of the core hole at the bottom of the pavement. To seal the bottom of the CHP device, an open-cell foam ring is compressed under the CHP device. By inflating a rubber tube between the outside of the CHP device ring and the core hole wall, the perimeter of the CHP device is sealed

against the core hole wall. About 20 to 25 psi of air pressure is used to inflate the rubber tube. Figure 25 shows the components of the CHP device, and Figure 26 shows the field setup.

Figure 25. CHP device and components

Figure 26. Core hole permeability testing under PCC pavement

Tests are performed by filling the permeameter with water and recording the head loss with time for 1-minute intervals. Test readings are taken intermittently over a period of about 30 minutes (after 1, 3, 6, 10, 15, and 30 minutes). Saturated hydraulic conductivity can be determined based on concepts provided in ASTM D6391-06.

The tests are proposed on a few selected test sections (6th St. South and 11th St. North) with and without the GCDL beneath the pavement layer and on a control section (8th St.) with a modified subbase layer where comparative permeability measurements were available on the modified subbase layer prior to paving.

AASHTO (1993) provides guidance on using hydraulic conductivity values to estimate the coefficient of drainage (C_d) design parameter based on pavement geometry (i.e., width of the pavement, maximum distance to the subdrain, cross slope, longitudinal slope), the thickness of the subbase layer, and the effective porosity of the subbase material. The calculation involves determining the time to drain a specified percentage of water out of the pavement system (AASHTO 1993). An Excel-based pavement drainage estimator developed at ISU (White et al. 2004, Vennapusa 2004) can be used based on the measured hydraulic conductivity values from the CHP tests.

Dynamic Cone Penetrometer Test

At each of the DCP test locations, a 1 in. diameter hole will be drilled in the pavement down to the bottom of the pavement layer (Figure 27). This hole will be used to verify the pavement layer thickness and perform a DCP test in the foundation layer. DCP testing will provide penetration resistance and CBR profiles with depth up to about 30 in. below pavement surface. The DCP test will be performed in accordance with ASTM D6951.

Figure 27. DCP test through a 1 in. diameter hole in the pavement layer

Assessment of Seasonal Variation in Modulus Values

Post-construction changes in saturation levels in the foundation layers are inevitable due to seasonal changes with wetting/drying or freezing/thawing. AASHTOWare Pavement ME Design addresses these seasonal variations through the Enhanced Climatic Integrated Model (EICM), which incorporates regional databases of climatic changes and assumed moisture variations and estimates their potential effects on moduli values through empirical equations (AASHTO 2015). The older version of the AASHTO pavement design (AASHTO 1993) addresses seasonal variations by assigning a modulus value for each season (i.e., winter, spring, summer, and fall). Other pavement design procedures (e.g., FAA 2009, PCA 1984) assume moduli values of materials when in saturated state in the design.

Regardless of the design method chosen, it is well known that modulus/stiffness properties are significantly influenced by the degree of saturation. The value assumed in the design is not a singular value but is a stress-dependent and moisture/saturation-dependent value.

In the proposed Phase IV testing plan, the field testing will be conducted during the spring thaw period, when the foundation layers are expected to be in their weakest condition, and in fall, when the foundation layers reach a stable condition in terms of moisture variations. On-site

temperature sensor results and Iowa Environmental Mesonet data will be used to determine the spring thaw time for testing.

AASHTOWare Pavement ME Design uses the EICM to apply empirical corrections in order to model seasonal variations in the resilient modulus values using matric suction parameters as inputs to the M_r constitutive universal model. There are varying degrees of complexity in determining the values of the needed material properties, the laboratory testing needed, and the uncertainties involved in implementing the models. One of the simpler approaches was proposed by Liang et al. (2008), which incorporates two suction parameters into the M_r constitutive universal model as follows:

$$M_r = k_1 P_a \left(\frac{\theta + \chi_w \psi_m}{P_a}\right)^{k_2} \left(\frac{\tau_{oct}}{P_a} + 1\right)^{k_3} \quad (2)$$

$$\chi_w = \left(\frac{(\psi_m)_b}{\psi_m}\right)^{0.55} \quad (3)$$

where M_r = resilient modulus (psi); P_a = atmospheric pressure (psi); θ = bulk stress (psi) = $\sigma_1 + \sigma_2 + \sigma_3$; $\sigma_2 = K_o \sigma_1$; $\sigma_3 = \sigma_2$; K_o = coefficient of lateral earth pressure at rest = $\nu/(1-\nu)$; ν = Poisson's ratio; τ_{oct} = octahedral shear stress (psi) = $\sqrt{(\sigma_1 - \sigma_2)^2 + (\sigma_2 - \sigma_3)^2 + (\sigma_3 - \sigma_1)^2} / 3$; k_1, k_2, and k_3= regression coefficients; χ_w = Bishop's parameter corresponding to a given moisture content or degree of saturation; ψ_m= matric suction at a given moisture content or degree of saturation; and $(\psi_m)_b$= air entry value or matric suction where air starts to enter the largest pores in the soil.

Liang et al. (2008) evaluated the model (equation [2]) for matric suction values greater than the air entry value (i.e., $\psi_m > (\psi_m)_b$), and therefore for $\chi_w > 1$. One advantage with using this approach is that the in situ M_r results from stress-dependent cyclic plate load tests can be modeled using equation (2) if the suction parameters (ψ_m and χ_w) are known for the test location. The suction parameters can be measured experimentally by developing soil-water characteristic curves (SWCCs) for the material and measuring the in situ moisture content and dry density. The experimental method involves performing filter paper method tests (ASTM D5298) on reconstituted samples compacted to different moisture contents and dry densities. Alternatively, SWCCs can be estimated following the empirical relationships provided in Zapata and Houston (2008) based on soil index properties and using the Fredlund and Xing (1994) model, which is used in AASHTOWare Pavement ME Design as shown below:

$$\theta_w = C(h) \times \left[\frac{\theta_{sat}}{\left[ln\left[2.7183 + \left(\frac{\psi_m}{a_f}\right)^{b_f}\right]\right]^{c_f}}\right] \quad (4)$$

$$C(h) = \left[1 - \frac{ln\left(1+\frac{\psi}{h_r}\right)}{ln\left(1+\frac{1.45\times10^5}{h_r}\right)}\right] \quad (5)$$

where ψ_m = matric suction (psi); θ_w = volumetric moisture content (decimal), which can be replaced with degree of saturation (decimal); θ_{sat} = volumetric moisture content (decimal) at the maximum degree of saturation, which can be replaced with the maximum degree of saturation (decimal) of the material; and a_f, b_f, c_f, and h_r = SWCC curve fitting parameters correlated with material gradation properties using a database of nonplastic granular materials (plasticity index = 0), as shown in equations (6) to (16), and plastic soils, as shown in equations (17) to (20).

Nonplastic granular soils:

$a_f = 1.14a_i - 0.5$ (Note: when a_f results in negative value, use $a_f = 1.0$) (6)

$$a_i = -2.79 - 14.1\,log(D_{20}) - 1.9\times10^{-6}P_{200}^{4.34} + 7\,log(D_{30}) + 0.055D_{100} \quad (7)$$

$$D_{100} = 10^{\left[\frac{40}{m_1}+log(D_{60})\right]} \quad (8)$$

$$m_1 = \frac{30}{[log(D_{90})-log(D_{60})]} \quad (9)$$

$$b_f = 0.936b - 3.8 \quad (10)$$

$$b = \left(5.39 - 0.29\,ln\left[P_{200}\left(\frac{D_{90}}{D_{10}}\right)\right] + 3D_0^{0.57} + 0.021P_{200}^{1.19}\right)\times m_1^{0.1} \quad (11)$$

$$D_0 = 10^{\left[\frac{-30}{m_2}+log(D_{30})\right]} \quad (12)$$

$$m_2 = \frac{20}{[log(D_{30})-log(D_{10})]} \quad (13)$$

$$c_f = 0.26e^{0.785\times c} + 1.4D_{10} \quad (14)$$

$$c = log(m_2^{1.15}) - \left(1 - \frac{1}{b_f}\right) \quad (15)$$

$$h_r = 100 \quad (16)$$

Plastic soils:

$$a_f = 32.835\left(ln(P_{200}\cdot PI)\right) + 32.438) \quad (17)$$

$$b_f = 1.421(P_{200} \cdot PI)^{0.3185} \quad (18)$$

$$c_f = -0.2154\left(ln(P_{200} \cdot PI)\right) + 0.7145 \quad (19)$$

$$h_r = 500 \quad (20)$$

where D_{10} = grain size corresponding to 10% passing by weight (mm); D_{20} = grain size corresponding to 20% passing by weight (mm); D_{30} = grain size corresponding to 30% passing by weight (mm); D_{60} = grain size corresponding to 60% passing by weight (mm); D_{90} = grain size corresponding to 90% passing by weight (mm); and P_{200} = percentage material passing the #200 sieve (expressed as decimals).

Gradation information available from Phase I construction will be reviewed, and additional samples as necessary will be obtained during field testing to determine these parameters.

SUMMARY

In this report, a field testing plan for the Phase IV evaluation is provided with details on the test sections to be evaluated, the number of tests recommended for each section, and the type of tests to be performed. The engineering measurement values to be obtained for each of the tests are summarized. A minimum recommended plan and a comprehensive plan are proposed, either of which can be used depending on funding levels approved. The testing program was developed with the goal of *direct* measurement of the in situ mechanistic input parameters that are necessary in AASHTOWare Pavement ME Design, along with the impacts of seasonal variations in the measurement values.

The pavement foundation layer stabilization methods that will be included in the Phase IV evaluation are as follows:

- Woven and nonwoven geotextiles at subgrade/subbase interface
- Triaxial and biaxial geogrids at subgrade/subbase interface
- PC stabilization of subgrade (10% PC)
- FA stabilization of subgrade (10% and 20% FA)
- PC stabilization of reclaimed subbase (reclaimed from existing granular subbase layer on site)
- PC + fiber stabilization of recycled subbase with white PP fibers
- PC + fiber stabilization of reclaimed subbase with black MF-PP fibers
- Mechanical stabilization (mixing subgrade with reclaimed subbase)
- Reclaimed subbase between MSB and subgrade
- High-energy impact compaction of subgrade

In addition, some test sections included a GCDL at the pavement/subbase interface, with a portion of those sections built without the drainage layer for comparison. Permeability tests are proposed in those areas for comparison.

APLT and CHP tests are selected as field testing methods to be used in the Phase IV evaluation. At each of the test locations, a DCP test will also be performed. These tests will be initiated in fall 2023 followed by testing in spring 2024, fall 2024, and spring 2025. On-site temperature sensor results and Iowa Environmental Mesonet data will be used to determine the spring thaw time for testing.

The APLTs will include a cyclic test performed on the pavement layer and a static and cyclic random loading test performed directly on the pavement foundation layer through a core hole in the pavement.

The engineering measurement values to be reported from the tests include the following:

- Composite resilient modulus ($M_{r\text{-}comp}$) for the pavement layer

- Layered modulus values for the pavement layer and the underlying foundation layers (modified subbase and subgrade layers)
- Permanent deformation forecasting regression model based on the number of loading cycles
- Modulus of subgrade reaction (*k*-values) for initial and reload cycles
- Ratio of reload to initial load *k*-value
- "Universal" model parameters for predicting M_r values along with permanent deformation model parameters

AASHTOWare Pavement ME Design uses the EICM to apply empirical corrections in order to model seasonal variations in the resilient modulus values using matric suction parameters as inputs to the M_r constitutive universal model. Empirical relationships to estimate the suction parameters using material gradation information are summarized in this report. Gradation information available from Phase I construction will be reviewed, and additional samples as necessary will be obtained during field testing to determine these parameters.

REFERENCES

ASTM D1195/D1195M-09. 2015. *Standard Test Method for Repetitive Static Plate Load Tests of Soils and Flexible Pavement Components, for Use in Evaluation and Design of Airport and Highway Pavements*. ASTM International, West Conshohocken, PA.

ASTM D1196/D1196M-12. 2016. *Standard Test Method for Nonrepetitive Static Plate Load Tests of Soils and Flexible Pavement Components, for Use in Evaluation and Design of Airport and Highway Pavements*. ASTM International, West Conshohocken, PA.

ASTM D6391-06. 2011. *Standard Test Method for Field Measurement of Hydraulic Conductivity Using Borehole Infiltration*. ASTM International, West Conshohocken, PA.

ASTM D5298. 2016. *Standard Test Method for Measurement of Soil Potential (Suction) Using Filter Paper*. ASTM International, West Conshohocken, PA.

ASTM D6951/D6951M-18. 2018. *Standard Test Method for Use of the Dynamic Cone Penetrometer in Shallow Pavement Applications*. ASTM International, West Conshohocken, PA.

AASHO. 1962. *The AASHO Road Test Report 5 – Pavement Research*. Special Report 61E, Publication No. 954. National Academy of Sciences, National Research Council, Washington, DC.

AASHTO. 1986. *AASHTO Guide for Design of Pavement Structures.* American Association of State Highway and Transportation Officials, Washington, DC.

AASHTO. 1993. *AASHTO Guide for Design of Pavement Structures.* American Association of State Highway and Transportation Officials, Washington, DC.

AASHTO. 2010. *Guide for the Local Calibration of the Mechanistic-Empirical Pavement Design Gide,* American Association of Highway and Transportation Officials, Washington, DC.

AASHTO. 2015. *Mechanistic-Empirical Pavement Design Guide: A Manual of Practice*, 2nd Edition. American Association of State Highway and Transportation Officials, Washington, DC.

Belle, G. 2008. *Statistical Rules of Thumb*, 2nd Edition. John Wiley & Sons, Hoboken, NJ.

Darter, M.I., L. Glover, H. Von Quintus, B. Bhattacharya, and J. Mallela. 2014. *Calibration and Implementation of the AASHTO Mechanistic Empirical Pavement Design Guide in Arizona*. SPR-606. Arizona Department of Transportation, Phoenix, AZ.

Gieselman, K., D. J. White, E. T. Cackler, J. Puls, and P. Vennapusa. 2023. *Demonstration of Innovative Technologies for Pavement Foundation Layer Construction: Pavement Foundation Mapping Projects*. TPF-5(478) MP (Interim). Iowa Department of Transportation, Ames, IA.

Fredlund, D. G., and A. Xing. 1994. Equations for the Soil-Water Characteristic Curve. *Canadian Geotechnical Journal*, Vol. 31, p 521-532. http://dx.doi.org/10.1139/t94-061.

FAA. 2009. *Airport Pavement Design and Evaluation*. AC150/5320-6F. U.S. Department of Transportation and Federal Aviation Administration, Washington, DC.

Liang, R. Y., S. Rabab'ah, and M. Khasawneh. 2008. Predicting Moisture-Dependent Resilient Modulus of Cohesive Soils Using Soil Suction Concept. *ASCE Journal of Transportation Engineering*, Vol. 134, No. 1, pp. 34–40.

Mallela, J., L. Glover, S. Sadasivam, B. Bhattacharya, M. Darter, and H. Von Quintus. 2013. *Implementation of the AASHTO Mechanistic-Empirical Pavement Design Guide for Colorado*. Report No. CDOT-2013-4. Colorado Department of Transportation, Denver, CO.

PCA. 1984. *Thickness design for concrete highway and street pavements*, Portland Cement Association, Skokie, IL.

Terzaghi, K. 1955. Evaluation of Coefficient of Subgrade Reaction, *Geotechnique*, Vol. 5, No. 4, pp. 297–326.

Teller, L. W., and E. C. Sutherland. 1935. The Structural Design of Concrete Pavements, Part 1, A Description of the Investigation. *Public Roads*, Vol. 16, No. 8.

Teller, L. W., and E. C. Sutherland. 1943. The Structural Design of Concrete Pavements, Part 5, An Experimental Study of the Westergaard Analysis of Stress Conditions in Concrete Pavements of Uniform Thickness. *Public Roads*, Vol. 23, No. 8.

U.S. Army Corps of Engineers. 1943. *Report of Special Field Bearing Tests on Natural Subgrade and Prepared Subbase Using Different Size Bearing Plates*. Ohio River Division, Office of the Division Engineer, Cincinnati Testing Laboratory Soils Division, U.S., Army Corps of Engineers, Mariemont, OH.

Vennapusa, P. 2004. Determination of Optimum Base Characteristics for Pavements. MS Thesis. Iowa State University, Ames, IA.

Vennapusa, P., D. J. White, M. Wayne, J. Kwon, A. Galindo, and L. García. 2018. In situ performance verification of geogrid-stabilized aggregate layer: Route-39 El Carbón–Bonito Oriental, Honduras case study. *International Journal of Pavement Engineering*, Vol. 21, No. 1, pp. 100–111.

White, D. J., P. Becker, P. Vennapusa, M. J. Dunn, and C. White. 2013. Assessing Soil Stiffness of Stabilized Pavement Foundations. *Transportation Research Record: Journal of the Transportation Research Board*, Vol. 2335, No. 1, pp. 99–109.

White, D. J., P. Vennapusa, and C. T. Jahren. 2004. *Determination of the Optimum Base Characteristics for Pavements*, Iowa DOT Project TR-482, Iowa Highway Research Board, Iowa Department of Transportation, Ames, IA.

White, D. J., and P. Vennapusa. 2014. *Optimizing Pavement Base, Subbase, and Subgrade Layers for Cost and Performance on Local Roads*. Center for Earthworks Engineering Research, Ames, IA.

White, D. J., and P. Vennapusa. 2017. In situ resilient modulus for geogrid-stabilized aggregate layer: A case study using automated plate load testing. *Transportation Geotechnics*, Vol. 11, pp. 120–132.

White, D. J., P. Vennapusa, P. Becker, J. Rodriguez, J. Zhang, and C. White. 2018. *Central Iowa Expo Pavement Test Sections: Pavement and Foundation Construction Testing and Performance Monitoring*. Center for Earthworks Engineering Research, Ames, IA.

White, D. J., P. Vennapusa, and T. Cackler. 2019a. *In Situ Modulus Measurement Using Automated Plate Load Testing for Statewide Mechanistic-Empirical Design Calibration*. Report No. ST-003. Iowa Department of Transportation, Ames, IA.

White, D. J., P. Vennapusa, and J. Siekmeier. 2019b. Cyclic Plate Load Testing for Assessment of Asphalt Pavements Supported on Geogrid Stabilized Granular Foundation. Eighth International Conference on Case Histories in Geotechnical Engineering, March 24–27, Philadelphia, PA.

Zapata, C. E., and W. N. Houston. 2008. *NCHRP Report 602: Calibration and Validation of the Enhanced Integrated Climatic Model for Pavement Design*. National Cooperative Highway Research Program, Washington, DC.

APPENDIX A. LIST OF PROJECT ENGINEERING PUBLICATIONS FROM PROJECT PHASES I THROUGH III

Technology Transfer Products

- Phase I Foundation Layer Construction Video (10 minutes) – Posted on YouTube
- Phase II Paving Video (10 minutes) – Posted on YouTube
- Tech Briefs (https://intrans.iastate.edu/research/completed/boone-county-expo-research-phase-i-granular-road-compaction-and-stabilization/)

1. Overview of Foundation Stabilization Technologies
2. Stiffness-Based QC/QA Testing
3. High Energy Impact Compaction
4. Roller-Integrated Compaction Monitoring of Subbase
5. Subgrade Stabilization using Geosynthetics
6. Fly Ash Stabilization of Subgrade
7. Cement Stabilization of Subgrade and Subbase
8. Cement Stabilization with Fiber Reinforcement of Subbase
9. Mechanical Stabilization of Subgrade
10. Geocell Confinement of Subbase Layer
11. Recycled Granular Material as Subbase

Technical Products

A. Final Report:

1. White, D.J., Vennapusa, P., Becker, P., Rodriguez, J., Zhang, J., White, C. (2018). *Central Iowa Expo Pavement Test Sections: Pavement and Foundation Construction Testing and Performance Monitoring*. IHRB Project TR-671. Iowa Department of Transportation, Ames, IA. https://intrans.iastate.edu/app/uploads/2018/03/Central_Iowa_Expo_pvmt_section_perf_w_cvr.pdf

B. Technical Articles:

1. White, D. J., Becker, P., Vennapusa, P., Dunn, M. White, C. (2013). "Assessing Soil Stiffness of Stabilized Pavement Foundations," Transportation Research Record: Journal of the Transportation Research Board, Vol. 2335. (Recipient of Best Paper Award by the Geology and Properties of Earth Materials Section). https://doi.org/10.3141/2335-11
2. Becker, P., White, D.J., Vennapusa, P., Dunn, M. (2014). "Freeze-Thaw Performance Assessment of Stabilized Pavement Foundations," Proc. of 93rd Annual Transportation Research Board Meeting, Paper ID14-5330, Washington, DC. https://trid.trb.org/view/1289994
3. White, D.J., Vennapusa, P. (2014). "Rapid In Situ Measurement of Hydraulic Conductivity for Granular Pavement Foundations," ASCE Geo-Congress 2014 Conference, Feb 23-26, Atlanta, GA. https://ascelibrary.org/doi/10.1061/9780784413272.292

4. Becker, P., White, D.J., Vennapusa, P., White, C., Zhang, J. (2015). "Performance Comparison of Recycled Pavement Foundation Layers," Transportation Research Record: Journal of the Transportation Research Board, Vol. 2335. https://doi.org/10.3141/2509-04
5. White, D.J., Vennapusa, P., Becker, P., Zhang, J., and Dunn, M. (2015). "Performance Assessment of Cement Stabilized, Polymer Fiber-Reinforced Pavement Foundation Layers," Geosynthetics 2015 Conference, Feb 15-18, Portland, OR. https://geosyntheticsconference.com/proceedings-archive-access/
6. Hu, J., Vennapusa, P., White, D.J., Beresnev, I. (2015). "Pavement thickness and stabilised foundation layer assessment using ground-coupled GPR," Nondestructive Testing and Evaluation, http://dx.doi.org/10.1080/10589759.2015.1111890.
7. Zhang, Y., Johnson, A., and White, D.J. (2016). "Laboratory Freeze-Thaw Assessment of Cement, Fly Ash, and Fiber Stabilized Pavement Foundation Materials," Cold Regions Science and Technology, Vol. 122, 50-57. https://www.sciencedirect.com/science/article/abs/pii/S0165232X15002657
8. Li, C., Ashlock, J., White, D., and Vennapusa, P. (2017). "Permeability and Stiffness Assessment of Paved and Unpaved Roads with Geocomposite Drainage Layers," Applied Sciences, Vol. 7, No. 718. https://www.mdpi.com/2076-3417/7/7/718
9. Zhang, Y., Horton, R., White, D.J., and Vennapusa, P. (2017). "Seasonal Frost Penetrations in Pavements with Multiple Layers," Journal of Cold Regions Engineering, Vol. 32, Issue 2. https://ascelibrary.org/doi/10.1061/%28ASCE%29CR.1943-5495.0000159

C. Thesis/Dissertations:

1. Becker, P. (2016). "The Central Iowa Expo site pavement foundation stabilization and paving project: An investigation into the influence of pavement foundation stiffness on pavement design, construction, and performance." Ph.D. Dissertation., Department of Civil, Construction, and Environmental Engineering, Iowa State University, Ames, IA. https://doi.org/10.31274/etd-180810-4733.
2. Zhang, Y. (2017). "Assessing seasonal performance, stiffness, and support conditions of pavement foundations." Ph.D. Dissertation, Department of Civil, Construction, and Environmental Engineering, Iowa State University, Ames, IA. https://doi.org/10.31274/etd-180810-5092
3. Hu, J. (2015). "Nondestructive field assessment of flexible pavement and foundation layers." MS Thesis, Department of Civil, Construction, and Environmental Engineering, Iowa State University, Ames, IA. https://doi.org/10.31274/etd-180810-3927

APPENDIX B. SUMMARY OF TEST SECTIONS AND PROPOSED PHASE IV TEST PLAN

PROPOSED MINIMUM SCOPE OF WORK

Street	Section	Station	Pavement	Subbase	Subgrade Improvement	FWD Test Measurements from Phase I Stud					Number of Proposed Test Measurements			
						Avg. Oct 2012 (E_{FWD}, MPa)	Avg. Apr 2013 (E, MPa)	Ratio of Oct 2012/April 2013	COV Oct 2012 (E_{FWD}, %)	COV Apr 2013 (E_{FWD}, %)	APLT Test A [Cyclic Test on HMA/PCC]	APLT Test C (Cyclic RDL on Foundation)	APLT Test B (Static Test)	CHP Test
1st	South	100+12.00 to 106+86.00	2 in. HMA + 4 in. HMA	6 in. (5.5 in. actual) MSB	12 in. compacted subgrade	163	22	7.4	34	17	0	0	0	0
	North	107+14.00 to 113+88.00	2 in. HMA + 4 in. HMA			98	17	5.8	39	11	0	0	0	0
2nd	South	200+12.00 to 206+86.00	2 in. HMA + 4 in. HMA	6 in. (6.1 in. actual) MSB[b]	12 in. mechanically stabilized subgrade	174	26	6.7	24	16	2	1	1	0
	North	207+14.00 to 213+88.00	2 in. HMA + 4 in. HMA			128	26	4.9	24	22	2	1	1	0
3rd	South	300+12.00 to 306+86.00	2 in. VMA + 4 in. VMA	1 in. MSB	6 in. geocell reinforced MSB, NW geotextile (no geotextile between 306+04.00 to 306+86.00)	44	16	2.8	42	10	0	0	0	0
	North	307+14.00 to 313+88.00	2 in. HMA + 4 in. HMA	2 in. MSB	4 in. geocell reinforced MSB, NW geotextile	37	18	2.1	19	12	0	0	0	0
4th	South	400+12.00 to 406+86.00	2 in. VMA + 4 in. VMA	6 in. (7.0 in. actual) MSB	woven geotextile	74	25	3.0	27	15	2	1	1	0
	North	407+14.00 to 413+88.00	2 in. VMA + 4 in. VMA	6 in. (7.0 in. actual) MSB	NW geotextile	95	23	4.1	28	58	2	1	1	0
5th	South	500+12.00 to 506+86.00	2 in. VMA + 4 in. VMA	6 in. (5.8 in. actual) MSE	biaxial geogrid	103	20	5.2	29	17	2	1	1	0
	North	507+14.00 to 513+88.00	2 in. VMA + 4 in. VMA	6 in. (5.8 in. actual) MSE	triaxial geogric	122	21	5.8	28	12	2	1	1	0
6th	South	4020+82.30 to 4026+65.49	6 in. PCC + GCDL	6 in. (4.5 to 5 in. actual) MSB	6 in. reclaimed subbase + 5% (5.5% actual) PC + 0.4% (0.5% actual) MF-PP fibers	246	116	2.1	21	21	2	1	1	0
		4020+21.30 to 4020+82.30	6 in. PCC + GCDL		6 in. reclaimed subbase + 0.4% (0.4% actual) MF-PP fibers						1	1	1	1
	North	4026+93.49 to 4032.85.49	6 in. PCC	6 in. (4.5 to 5 in. actual) MSB	6 in. reclaimed subbase + 5% (5.6% actual) PC + 0.4% (0.5% actual) PP fibers	285	140	2.0	17	35	2	1	1	1
		4032+85.49 to 4033+67.49	6 in. PCC		6 in. reclaimed subbase + 0.4% (0.5% actual) PP fibers						1	1	1	0
7th	South	700+12.00 to 706+86.00	2 in. HMA + 4 in. HMA	6 in. (5.5 in. actual) MSB	6 in. reclaimed subbase + 5% (5.2% actual) PC	176	91	1.9	32	18	2	0	0	0
	North	707+14.00 to 713+88.00	2 in. HMA + 4 in. HMA	6 in. (5.5 in. actual) MSB	6 in. reclaimed subbase + 5% (6.2% actual) PC	280	123	2.3	16	16	2	1	1	0
8th	South	800+12.00 to 806+86.00	2 in. HMA + 4 in. HMA	6 in.(6.0 in. actual) MSE	Compacted subgrade	63	13	4.8	28	19	2	1	1	1
	North	807+14.00 to 813+88.00	2 in. HMA + 4 in. HMA	6 in.(6.0 in. actual) MSE	Compacted subgrade	123	11	11.2	66	19	2	1	1	1
9th	South	900+12.00 to 906+86.00	2 in. VMA + 4 in. VMA	6 in.(6.0 in. actual) MSE	6 in. reclaimed subbase	195	44	4.4	18	11	2	0	0	0
	North	907+14.00 to 913+88.00	2 in. HMA + 4 in. HMA	6 in.(6.0 in. actual) MSE	6 in. reclaimed subbase	168	41	4.1	29	23	2	1	1	0
10th	South	1000+12.00 to 1006+86.00	2 in. VMA + 4 in. VMA	6 in. (5.5 in. actual) MSB	**EXISTING SUBGRADE [CONTROL]**	43	14	3.1	41	23	2	1	1	0
	North	1007+14.00 to 1013+88.00	2 in. VMA + 4 in. VMA	6 in. (5.5 in. actual) MSE	12 in. compacted subgrade	103	17	6.1	27	23	2	1	1	0
11th	South	1100+12.00 to 1106+86.00	2 in. VMA + 4 in. VMA	6 in.(6.0 in. actual) MSB	12 in. 20% (22.3% actual) Port Neal FA stabilized subgrade	324	54	6.0	21	54	2	1	1	0
	North	1107+14.00 to 1108+00 (approx.)	2 in. VMA + 4 in. VMA	6 in.(6.0 in. actual) MSB	12 in. 10% (11.4% actual) PC stabilized subgrade	507	159	3.2	28	23	2	0	0	1
		1108+00 to 1113+88.00	2 in. VMA + 4 in. VMA + GCDL								2	1	1	1
12th	South	1200+12.00 to 1204+46.00	2 in. HMA + 4 in. HMA	6 in. (6.0 in. actual) MSB	12 in. 10% (10% actual) Port Neal FA stabilized subgrade	237	29	8.2	33	48	2	1	1	0
		1204+46.00 to 1206+86.00			12 in. 10% (10% actual) Muscatine FA stabilized subgrade						2	1	1	0
	North	1207+14.00 to 1213+88.00	2 in. HMA + 4 in. HMA	6 in. (5.7 in. actual) MSB[b]	12 in. 15% (15.8% actual) Ames FA stabilized subgrade	321	39	8.2	15	29	2	1	1	0
North Ave	West	3000+02.50 to 3002+02.50	6 in. PCC	9 in. MSB	6 in. reclaimed subbase, biaxial geogrid						0	0	0	0
	West	3002+02.50 to 3004+02.50	6 in. PCC	9 in. MSB	6 in. reclaimed subbase, triaxial geogrid						0	0	0	0
	East	3004+02.50 to 3023+38.14	6 in. PCC	9 in. MSB	6 in. reclaimed subbase						0	0	0	0
South Ave.	West[e]	1001+00.00 to 1003+00.00	6 in. PCC	9 in. MSB[f]	6 in. reclaimed subbase, biaxial geogrid						0	0	0	0
		1003+00.00 to 1005+00.00	6 in. PCC		6 in. reclaimed subbase, biaxial geogrid						0	0	0	0
		1005+00.00 to 1009+06.08	6 in. PCC		6 in. reclaimed subbase						0	0	0	0
South Ave.	East[e]	1009+94.00 to 1011+94.00	6 in. PCC	9 in. MSB[f]	6 in. reclaimed subbase, biaxial geogrid						0	0	0	0
		1011+94.00 to 1013+94.00	6 in. PCC		6 in. reclaimed subbase, biaxial geogrid						0	0	0	0
		1013+94.00 to 1023+39.91	6 in. PCC		6 in. reclaimed subbase						0	0	0	0
Central Ave.	East/West	2000+01.43 to 2023+39.59	6 in. PCC	9 in. MSB[f]	6 in. reclaimed subbase						0	0	0	0
										TOTAL	46	21	21	6

PROPOSED COMPREHENSIVE SCOPE OF WORK

Street	Section	Station	Pavement	Subbase	Subgrade Improvement	FWD Test Measurements from Phase I Study					Number of Proposed Test Measurements			
						Avg. Oct 2012 (E_{FWD}, MPa)	Avg. Apr 2013 (E, MPa)	Ratio of Oct 2012/April 2013	COV Oct 2012 (E_{FWD}, %)	COV Apr 2013 (E_{FWD}, %)	APLT Test A [Cyclic Test on HMA/PCC]	APLT Test C (Cyclic RDL on Foundation)	APLT Test B (Static Test)	CHP Test
1st	South	100+12.00 to 106+86.00	2 in. HMA + 4 in. HMA	6 in. (5.5 in. actual) MSB	12 in. compacted subgrade	163	22	7.4	34	17	0	0	0	0
	North	107+14.00 to 113+88.00	2 in. HMA + 4 in. HMA			98	17	5.8	39	11	0	0	0	0
2nd	South	200+12.00 to 206+86.00	2 in. HMA + 4 in. HMA	6 in. (6.1 in. actual) MSB[b]	12 in. mechanically stabilized subgrade	174	26	6.7	24	16	3	1	1	0
	North	207+14.00 to 213+88.00	2 in. HMA + 4 in. HMA			128	26	4.9	24	22	3	1	1	0
3rd	South	300+12.00 to 306+86.00	2 in. WMA + 4 in. WMA	1 in. MSB	6 in. geocell reinforced MSB, NW geotextile (no geotextile between 306+04.00 to 306+86.00)	44	16	2.8	42	10	0	0	0	0
	North	307+14.00 to 313+88.00	2 in. HMA + 4 in. HMA	2 in. MSB	4 in. geocell reinforced MSB, NW geotextile	37	18	2.1	19	12	0	0	0	0
4th	South	400+12.00 to 406+86.00	2 in. WMA + 4 in. WMA	6 in. (7.0 in. actual) MSB	woven geotextile	74	25	3.0	27	15	6	1	1	0
	North	407+14.00 to 413+88.00	2 in. WMA + 4 in. WMA	6 in. (7.0 in. actual) MSB	NW geotextile	95	23	4.1	28	58	6	1	1	0
5th	South	500+12.00 to 506+86.00	2 in. WMA + 4 in. WMA	6 in. (5.8 in. actual) MSE	biaxial geogrid	103	20	5.2	29	17	6	1	1	0
	North	507+14.00 to 513+88.00	2 in. WMA + 4 in. WMA	6 in. (5.8 in. actual) MSE	triaxial geogric	122	21	5.8	28	12	6	1	1	0
6th	South	4020+82.30 to 4026+65.49	6 in. PCC + GCDL	6 in. (4.5 to 5 in. actual) MSB	6 in. reclaimed subbase + 5% (5.5% actual) PC + 0.4% (0.5% actual) MF-PP fibers	246	116	2.1	21	21	4	1	1	0
		4020+21.30 to 4020+82.30	6 in. PCC + GCDL		6 in. reclaimed subbase + 0.4% (0.4% actual) MF-PP fibers						2	1	1	1
	North	4026+93.49 to 4032.85.49	6 in. PCC	6 in. (4.5 to 5 in. actual) MSB	6 in. reclaimed subbase + 5% (5.6% actual) PC + 0.4% (0.5% actual) PP fibers	285	140	2.0	17	35	4	1	1	1
		4032+85.49 to 4033+67.49	6 in. PCC		6 in. reclaimed subbase + 0.4% (0.5% actual) PP fibers						2	1	1	0
7th	South	700+12.00 to 706+86.00	2 in. HMA + 4 in. HMA	6 in. (5.5 in. actual) MSB	6 in. reclaimed subbase + 5% (5.2% actual) PC	176	91	1.9	32	18	3	0	0	0
	North	707+14.00 to 713+88.00	2 in. HMA + 4 in. HMA	6 in. (5.5 in. actual) MSB	6 in. reclaimed subbase + 5% (6.2% actual) PC	280	123	2.3	16	16	3	1	1	0
8th	South	800+12.00 to 806+86.00	2 in. HMA + 4 in. HMA	6 in.(6.0 in. actual) MSE	Compacted subgrade	63	13	4.8	28	19	2	1	1	1
	North	807+14.00 to 813+88.00	2 in. HMA + 4 in. HMA	6 in.(6.0 in. actual) MSE	Compacted subgrade	123	11	11.2	66	19	2	1	1	1
9th	South	900+12.00 to 906+86.00	2 in. WMA + 4 in. WMA	6 in.(6.0 in. actual) MSE	6 in. reclaimed subbase	195	44	4.4	18	11	3	0	0	0
	North	907+14.00 to 913+88.00	2 in. HMA + 4 in. HMA	6 in.(6.0 in. actual) MSE	6 in. reclaimed subbase	168	41	4.1	29	23	3	1	1	0
10th	South	1000+12.00 to 1006+86.00	2 in. WMA + 4 in. WMA	6 in. (5.5 in. actual) MSB	**EXISTING SUBGRADE [CONTROL]**	43	14	3.1	41	23	6	1	1	0
	North	1007+14.00 to 1013+88.00	2 in. WMA + 4 in. WMA	6 in. (5.5 in. actual) MSE	12 in. compacted subgrade	103	17	6.1	27	23	6	1	1	0
11th	South	1100+12.00 to 1106+86.00	2 in. WMA + 4 in. WMA	6 in.(6.0 in. actual) MSB	12 in. 20% (22.3% actual) Port Neal FA stabilized subgrade	324	54	6.0	21	54	6	1	1	0
	North	1107+14.00 to 1108+00 (approx.)	2 in. WMA + 4 in. WMA	6 in.(6.0 in. actual) MSB	12 in. 10% (11.4% actual) PC stabilized subgrade	507	159	3.2	28	23	2	0	0	1
		1108+00 to 1113+88.00	2 in. WMA + 4 in. WMA + GCDL								4	1	1	1
12th	South	1200+12.00 to 1204+46.00	2 in. HMA + 4 in. HMA	6 in. (6.0 in. actual) MSB	12 in. 10% (10% actual) Port Neal FA stabilized subgrade	237	29	8.2	33	48	3	1	1	0
		1204+46.00 to 1206+86.00			12 in. 10% (10% actual) Muscatine FA stabilized subgrade						3	1	1	0
	North	1207+14.00 to 1213+88.00	2 in. HMA + 4 in. HMA	6 in. (5.7 in. actual) MSB[b]	12 in. 15% (15.8% actual) Ames FA stabilized subgrade	321	39	8.2	15	29	6	1	1	0
North Ave.	West	3000+02.50 to 3002+02.50	6 in. PCC	9 in. MSB	6 in. reclaimed subbase, biaxial geogrid						0	0	0	0
	West	3002+02.50 to 3004+02.50	6 in. PCC	9 in. MSB	6 in. reclaimed subbase, triaxial geogrid						0	0	0	0
	East	3004+02.50 to 3023+38.14	6 in. PCC	9 in. MSB	6 in. reclaimed subbase						0	0	0	0
South Ave.	West[e]	1001+00.00 to 1003+00.00	6 in. PCC	9 in. MSB[f]	6 in. reclaimed subbase, biaxial geogrid						0	0	0	0
		1003+00.00 to 1005+00.00	6 in. PCC		6 in. reclaimed subbase, biaxial geogrid						0	0	0	0
		1005+00.00 to 1009+06.08	6 in. PCC		6 in. reclaimed subbase						0	0	0	0
South Ave.	East[e]	1009+94.00 to 1011+94.00	6 in. PCC	9 in. MSB[f]	6 in. reclaimed subbase, biaxial geogrid						0	0	0	0
		1011+94.00 to 1013+94.00	6 in. PCC		6 in. reclaimed subbase, biaxial geogrid						0	0	0	0
		1013+94.00 to 1023+39.91	6 in. PCC		6 in. reclaimed subbase						0	0	0	0
Central Ave.	East/West	2000+01.43 to 2023+39.59	6 in. PCC	9 in. MSB[f]	6 in. reclaimed subbase						0	0	0	0
										TOTAL	94	21	21	6

THE INSTITUTE FOR TRANSPORTATION IS THE FOCAL POINT FOR TRANSPORTATION AT IOWA STATE UNIVERSITY.

InTrans centers and programs perform transportation research and provide technology transfer services for government agencies and private companies;

InTrans contributes to Iowa State University and the College of Engineering's educational programs for transportation students and provides K–12 outreach; and

InTrans conducts local, regional, and national transportation services and continuing education programs.

IOWA STATE UNIVERSITY

Visit **InTrans.iastate.edu** for color pdfs of this and other research reports.